



Energy, Mines and  
Resources Canada

Energie, Mines et  
Ressources Canada

### CANMET

Canada Centre  
for Mineral  
and Energy  
Technology

Centre canadien  
de la technologie  
des minéraux  
et de l'énergie

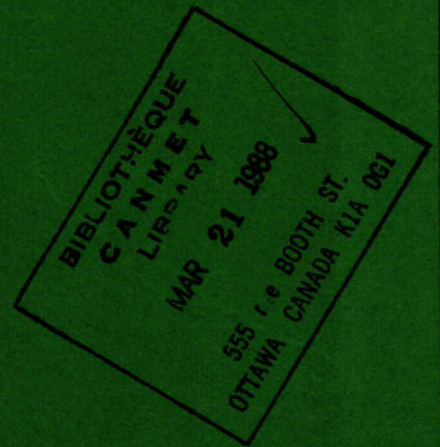
MRL 87-118 (TR)

ROCKBURST MECHANICS

D.G.F. HEDLEY

ELLIOT LAKE LABORATORY

MARCH 1987



This document is an unclassified  
report prepared by an author  
to...  
...  
...  
...  
...  
...  
(CANMET)

Ce document est un rapport  
non classifié préparé et rédigé  
par un auteur pour le compte de  
...  
...  
...  
...  
...  
...  
L'Agence nationale canadienne de  
l'information des minéraux et de  
l'énergie (CANMET)

69pp

MINING RESEARCH LABORATORIES  
DIVISION REPORT MRL 87-118 (TR)

MICROMEDIA

7993365

ROCKBURST MECHANICS

by

D.G.F.Hedley\*

SUMMARY

An energy balance approach is used to evaluate the causes and mechanisms of rockbursts. The damage caused by a rockburst is due to the seismic energy component which radiates out from the source. For elastic conditions, involving no rock fracturing, the amount of seismic energy liberated is dependent on the size of the mining steps. There are three broad categories of mining steps: infinitesimal, incremental and bulk methods. Examples would include tunnel borers, cut-and-fill techniques and blasthole stoping, respectively. For a given set of conditions there is an increasing amount of seismic energy liberated the larger the mining step and most Canadian mines employ either incremental or bulk methods.

In addition to the release of energy from purely elastic reactions, significant amounts of energy can be liberated during failure of the rock. Three types of rockbursts can be identified; strain, pillar, and fault-slip bursts. Strain bursts are caused by high stress concentrations. The source of the liberated energy is a combination of part of the stored strain energy in the failed rock, a change of potential energy of the rock mass, and, in some cases minor slippage along rock contacts. For pillar bursts the predominant source of seismic energy is the sudden change in potential energy of the rock mass. The source of energy in fault-slip bursts is the stored strain energy in the surrounding rock mass. A strong characteristic of the three types of rockbursts is their seismic efficiency, which is the proportion of the total energy release which is liberated seismically. Fault-slip bursts have a typical seismic efficiency of 1-10%, strain energy bursts 30-60%, and pillar bursts 70-90%. The amount of damage observed for the various rockburst types, of comparable magnitude, are also in the same order.

Whether pillars or faults fail violently or not is dependent on the

---

Key words: Rockbursts; Energy; Strain bursts; Pillar bursts; Fault-slip bursts

\*Senior Research Scientist, Elliot Lake Laboratory, CANMET, Energy, Mines and Resources Canada, Elliot Lake, Ontario.

loading stiffness compared to the stiffness of the rock after failure. For pillar bursts, the stored strain energy within the pillar is consumed in the fracturing process and the violence of the failure comes from the energy in the loading system (i.e., rock mass). Also it is misleading to consider pillars in isolation as equivalent to a single rock specimen in a compression testing machine. It has been demonstrated that the violent failure of pillars is dependent on the stiffness matrix of the loading system compared to the stiffness matrix of all the pillars in a panel and in the some cases the whole mine.

This report is a draft chapter of a "Rockburst Handbook for Canadian Hardrock Mines", being produced under the Canada/Ontario/Industry Rockburst Project.

## MECANISMES DES COUPS DE TOIT

par

D.G.F. Hedley

## SOMMAIRE

Une analyse énergétique est utilisée pour évaluer les causes et les mécanismes des coups de toit. Les dommages causés par ces derniers sont reliés à l'énergie sismique radiée à partir de la source. Pour des conditions élastiques impliquant aucune fracturation du roc, la quantité d'énergie libérée dépend de l'ampleur de chaque portion de roc excavé. On dénote trois grandes catégories d'excavations minières; infinitésimale, par abattage successif et par abattage de masse. Une illustration de ceci serait par exemple les perforatrices à tunnel, les techniques d'excavation par coupe et remblai et les méthodes d'abattage par trou de mine. Dans certaines conditions données, il se produit une augmentation de l'énergie sismique libérée comme par exemple lorsque de larges volumes de roc sont excavés. Tel est le cas de la plupart des mines Canadiennes qui emploient soit des techniques d'excavation par coupe et remblai ou les méthodes d'abattage par trou de mine.

En plus de l'énergie libérée à partir d'une réaction purement élastique, une quantité significative d'énergie peut aussi être libérée lors de la fracturation du roc. Trois catégories de coups de toit peuvent ainsi être identifiées; il y a celle reliée à la déformation du roc, celle reliée aux piliers de support et finalement celle reliée aux glissements de failles. Les coups de toit reliés à la déformation du roc sont causés par de grandes concentrations de contraintes. L'origine de l'énergie libérée est une combinaison de l'énergie de déformation emmagasinée dans la roche fracturée de même que du changement dans l'énergie potentielle de la masse rocheuse et, dans certains cas, du glissement mineur le long des contacts rocheux. Quant aux coups de toit reliés aux piliers, la source prédominante d'énergie sismique provient du changement soudain de l'énergie potentielle de la masse rocheuse et, dans certains cas, du glissement mineur le long des contacts rocheux.

La source d'énergie des coups de toit reliés aux glissements de failles réside dans l'énergie de déformation emmagasinée dans la masse rocheuse environnante. La principale caractéristique de ces trois types de coup de toit a trait à leur efficacité sismique c'est-à-dire à la proportion de l'énergie totale libérée qui est dissipée sous forme d'énergie sismique. Les coups de toit reliés aux glissements de failles ont une efficacité sismique de l'ordre de 1% à 10% alors qu'elle est de 30% à 60% pour les coups de toit reliés à la déformation du roc et de 70% à 90% pour les piliers. A magnitude comparable, la quantité de dommage observée pour ces différents types de coups de toit est du même ordre de grandeur.

Les piliers ou les failles se fracturent violemment ou non dépendamment de la rigidité du chargement par rapport à celle du roc pendant le processus d'après-fracturation. Pour les coups de toit reliés aux piliers de support, l'énergie de déformation emmagasinée à l'intérieur du pilier est consumée dans le processus de fracturation et la violence de la fracturation est causée par l'énergie emmagasinée dans le système de chargement (i.e. la masse rocheuse). De plus, il est trompeur de considérer les piliers isolément c'est-à-dire en les comparant individuellement à un échantillon de roc unique mis en compression. Au contraire, il a été prouvé que la rupture violente des piliers est reliée à la matrice de rigidité du système de chargement versus celle de l'ensemble de tous les piliers compris à l'intérieur d'un panneau d'extraction voire même, dans certains cas, de la mine entière.

Ce rapport constitue un chapitre préliminaire au manuel sur les coups de toit dans les mines Canadiennes à roche dure qui sera produit par "CANADA/ONTARIO/INDUSTRY ROCKBURST PROJECT".

## CONTENTS

	<u>Page</u>
SUMMARY .....	i
SOMMAIRE .....	iii
INTRODUCTION .....	1
ENERGY BALANCE .....	1
CALCULATION OF ENERGY COMPONENTS .....	5
INCREMENTAL VERSUS BULK MINING .....	8
TYPES OF ROCKBURSTS .....	12
Strain Bursts .....	13
Pillar Bursts .....	18
Fault-Slip Bursts .....	23
REFERENCES .....	29
APPENDIX .....	A-31

## TABLES

<u>No.</u>		
1.	Energy components in a blasthole stope in (MJ/m in length) .....	9
2.	Energy components for three 1 m slices on the last cut (in MJ/m in length) .....	11
3.	Energy components for a burst in a shaft (in MJ/m in length) ...	18
4.	Energy components for partial and complete pillar failure (in MJ/m in length) .....	19

## FIGURES

1.	Energy components when one specimen is removed from a press under constant load .....	3
2.	Section through a tabular excavation showing volumetric convergence and stress components (after Ortlepp 1983) .....	3
3.	Variation in how energy is released with number of mining steps (after Salamon 1983) .....	10
4.	Blasthole stoping .....	10
5.	Energy components per cut during mining of a vertical stope ...	10
6.	Violent and non-violent failure in soft and stiff testing machines .....	15
7.	Release of stored strain energy due to loss of confinement ....	15
8.	Stress-displacement characteristics of brittle and soft rocks..	17

9. Rockburst in a rectangular shaft .....	17
10. Stope and pillar model with two stages of pillar failure .....	17
11. Factors affecting loading stiffness .....	17
12. Factors affecting the post-failure stiffness of pillars .....	22
13. Multiple specimen testing .....	22
14. Load-displacement history of two specimens and aluminum pillar loaded simultaneously .....	22
15. Displacement, time, shear stress history of fault-slip model ..	24
16. Estimation of fault-slip parameters .....	24

## INTRODUCTION

Since rockbursts are the result of a violent release of energy it is natural that an analysis of energy is used to explain the mechanics of violent rock failure. Mechanical energy is a force acting through a displacement. In the "International System of Units" energy is calculated in terms of joules (J) which are newton-metres (N.m). In the "Imperial System" the equivalent units are foot-pound-force (1 ft-lb = 1.36 J).

Initially only the energy stored within the rock was considered as the source of the liberated energy. Later it was realized that there was a change in potential energy of the surrounding rock mass due to mining operations. This led to the concept of an energy balance, which was originally developed by Cook (1967) and later refined by Salamon (1974, 1984).

## ENERGY BALANCE

When a mining excavation is enlarged the surrounding rock mass moves towards the excavation resulting in a change in potential energy ( $W_t$ ). The rock removed during enlargement also contained stored strain energy ( $U_m$ ). The term ( $W_t + U_m$ ) represents the energy entering the mining operation as a result of the enlargement. This energy has to be dissipated somehow.

Stresses acting on the rock which was removed are transferred to the surrounding rock mass increasing its stored strain energy ( $U_c$ ). If the excavations are internally supported (e.g., backfill, cribs, posts) then some energy is absorbed in deforming the support ( $W_s$ ). Any excess energy is normally referred to as released energy ( $W_r$ ). From the law of conservation of energy:

$$W_t + U_m = U_c + W_s + W_r \quad \text{Eq 1}$$

In this analysis it is assumed that the rock behaves elastically and no



energy is consumed in fracturing or non-elastic deformation.

There are a number of ways in which energy can be released. The stored strain energy ( $U_m$ ) in the removed rock is obviously released. If the rock was removed instantaneously there would be oscillations in the rock mass. Equilibrium would be attained through damping and seismic (i.e., kinetic) energy ( $W_k$ ) would be dissipated in the process. For elastic conditions there are no further alternatives, hence:

$$W_r = U_m + W_k \quad \text{Eq 2}$$

It is the seismic energy ( $W_k$ ) which is recorded by mine microseismic systems, and it is this energy component which is responsible for the damage caused by a rockburst. From Equations 1 and 2:

$$W_k = W_t - (U_c + W_s) \quad \text{Eq 3}$$

For the case of unsupported excavations there is an inter-relationship between the energy components. This can be demonstrated by a simple example of two identical specimens under a constant load in a press, as shown in Figure 1(a). Both specimens would contain equal stored strain energy ( $U_m$ ) as identified in Figure 1(b). If one specimen was removed, while still maintaining constant load, then the stress on the remaining specimen would double as would the displacement between the platens. The stored strain energy ( $U_m$ ) in the removed specimen would be released (i.e., removed from the system) and the remaining specimen would carry the increase in stored strain energy ( $U_c$ ). The platens of the press would follow the displacement of the remaining specimen, with a resultant change in potential energy ( $W_t$ ). Areas representing various energy components are shown in Figure 1(b), with the following relationships:

$$U_c = 2U_m + U_1 \quad \text{Eq 4}$$

$$W_t = 2(U_m + U_1) \quad \text{Eq 5}$$

$$W_r = U_m + U_1 = W_t/2 \quad \text{Eq 6}$$

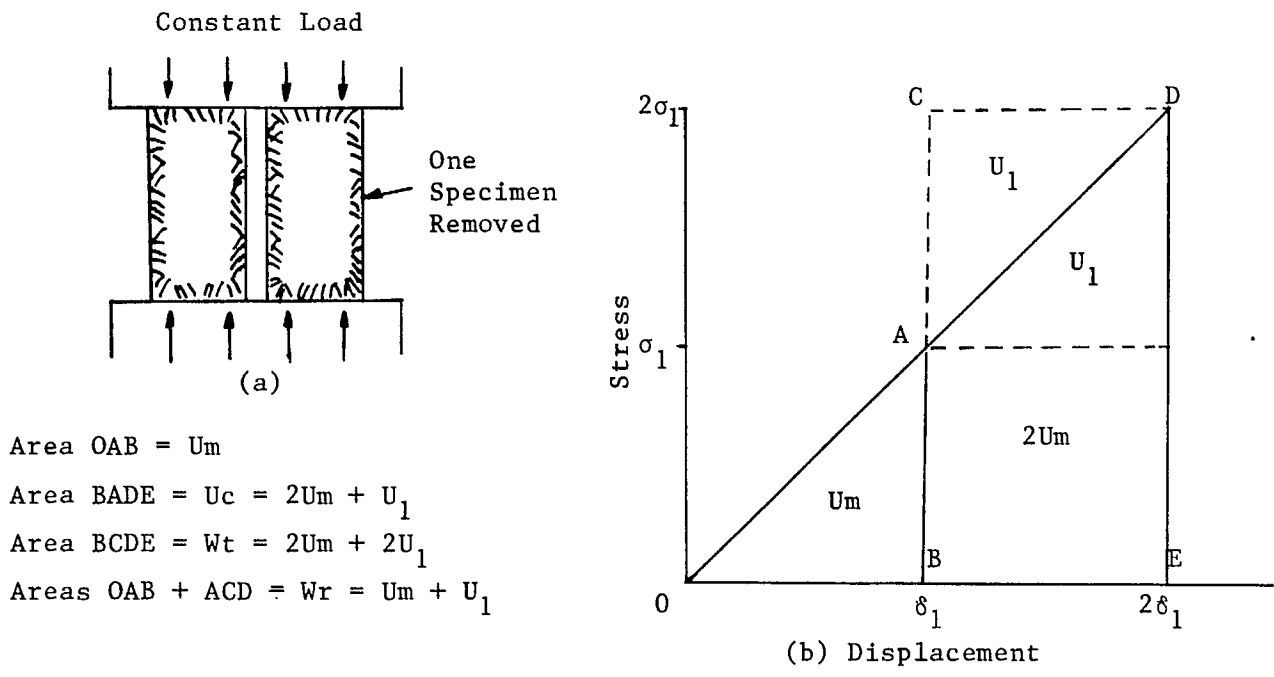


Fig. 1 - Energy components when one specimen is removed from a press under constant load.

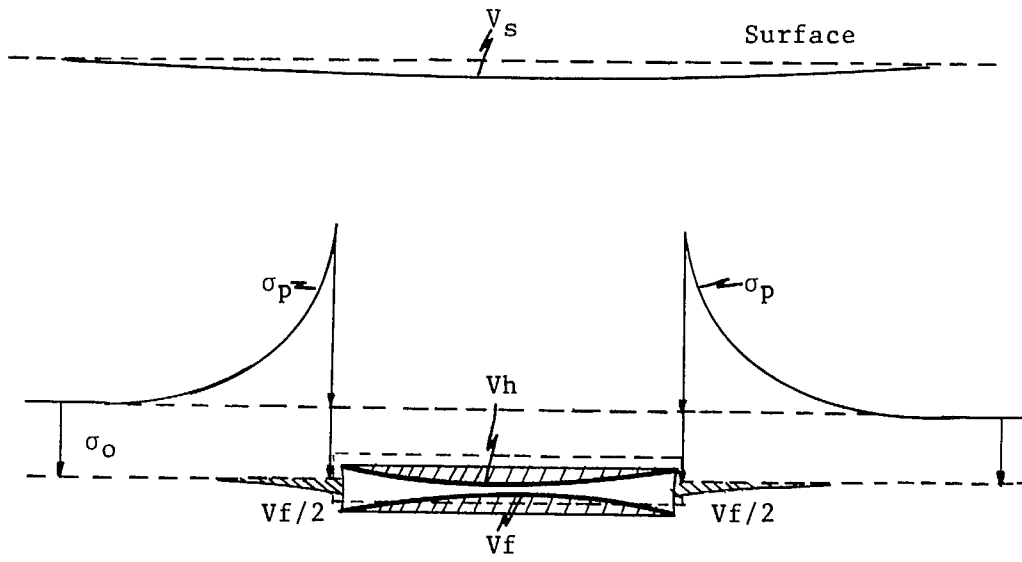


Fig. 2 - Section through a tabular excavation showing volumetric convergence and stress components (after Ortlepp 1933).

$$W_k = U_1 \quad \text{Eq 7}$$

where ( $U_1$ ) is the increase in stored strain energy if the stress increase had occurred on an unstressed specimen. Salamon (1974) has shown, for elastic conditions, that Equations 4, 5, 6 and 7 apply to any mining configuration. Also, when mining takes place in very small steps the limiting conditions are:

$$\Delta W_t = \Delta U_c, \quad \Delta W_r = \Delta U_m \quad \text{and} \quad \Delta W_k = 0 \quad \text{Eq 8}$$

Some fundamental deductions can be made from these energy relationships:

- a) Without support, all the energy components can be expressed in terms of two parameters ( $U_m$ ) and ( $U_1$ ). It is relatively easy to calculate these parameters using a variety of numerical models.
- b) When mining takes place in very small steps the process is stable and no seismic energy is released. In some cases this is contradictory, since many mines employ incremental methods but still experience rockbursts. However, this means that some other sources of energy are being liberated due to non-elastic conditions, either fracturing of a pillar or slippage along a fault.
- c) The change in potential energy ( $W_t$ ) is the driving force behind the other energy components. If it can be reduced the other energy components are correspondingly reduced.
- d) Support, such as backfill, has two beneficial effects. It will reduce the change in potential energy by reducing volumetric closure in the excavations and by absorbing energy, less energy is available to be released as seismic energy.

There are some other energy terms in common use. Energy release rate is the stored strain energy in the rock to be removed per unit area ( $\Delta U_m / \Delta A$ ). It is used in South African gold mines to rank rockburst potential of various mining layouts. There is a strong statistical relationship between energy

release rate and damage, in these mines (Hodgson and Joughin, 1967). Its use stems from Equation 8 and the concept of mining in very small steps.

Seismic efficiency is the ratio ( $W_k/W_r$ ) and is usually expressed as a percentage. For a given set of circumstances the higher the proportion of energy released as seismic energy the greater the rockburst potential.

Support efficiency is the ratio ( $W_s/W_r$ ), again as a percentage. The greater the proportion of energy absorbed by the support medium the less the rockburst potential.

#### CALCULATION OF ENERGY COMPONENTS

For simple geometrical mine openings it is possible to estimate the energy components using closed-form or approximate solutions. This has the benefit of identifying the parameters controlling the energy components. Complex mining geometry and multiple openings usually require more sophisticated numerical modelling techniques. A two-dimensional boundary element model (EXENBRAY), which incorporates Salamon's (1984) energy equations, is given in the Appendix.

Thin tabular excavations have been examined in detail in a number of publications. Figure 2 shows an isolated, horizontal narrow stope which prior to mining is subjected to a gravitational stress ( $\sigma_0$ ). After mining the vertical stress on the hanging wall and footwall of the stope is zero, and an equivalent stress is transferred to the abutments. The hanging wall subsides downwards with a volumetric convergence ( $V_h$ ), whereas the footwall lifts upwards with a volumetric convergence ( $V_f$ ). The former represents a loss of potential energy and the latter a gain in potential energy, relative to the centre of the Earth. However, the increase in stress on the abutments depresses the footwall plane by an identical volume as the uplift of the footwall in the stope. Consequently, the net change in potential energy of

the footwall is zero. Moreover, the hanging wall around the stope moves down by the same amount as the footwall is depressed. Thus the net volumetric convergence ( $V_c$ ) of the hanging wall is the sum of the hanging wall and footwall convergence in the stope, which is relatively easy to calculate:

$$V_c = V_h + V_f = V_s \quad \text{Eq 9}$$

For elastic conditions this volumetric stope closure also equals the volumetric subsidence ( $V_s$ ) of the surface, although the latter is spread over a much larger area.

The change in potential energy of the hanging wall can now be expressed by:

$$W_t = \sigma_o V_c \quad \text{Eq 10}$$

This equation is a valid approximation for thin tabular stopes. For more three-dimensional openings the change in horizontal potential energy (WH) as well as gravitational energy (WG) have to be accounted for:

$$W_t = W_G + W_H \quad \text{Eq 11}$$

and, 
$$W_t = \sigma_o V_c + \sigma_a V_a + \sigma_b V_b \quad \text{Eq 12}$$

where,  $\sigma_a, \sigma_b$  = horizontal stresses

$V_a, V_b$  = volumetric convergence of the vertical walls.

Stopes in tabular deposits, of any orientation, can be considered as thin slits with rigid abutments. The convergence distribution across an isolated stope can be approximated by (Salamon, 1968):

$$C = \frac{4(1-\nu^2)\sigma_o}{E} \left( 1 + \frac{\chi \sin \alpha}{2H} \right) \sqrt{s^2 - \chi^2} \quad \text{Eq 13}$$

where,  $C$  = hanging wall to footwall convergence

$E$  = elastic modulus

$\nu$  = Poisson's ratio

$\sigma_o$  = virgin stress perpendicular to the orebody

$\alpha$  = dip of orebody relative to horizontal

H = depth below surface to stope centre

s = half span of stope

$\chi$  = distance from centre of span ( $-s \leq \chi \leq s$ )

Assuming the principal stresses are vertical and horizontal the perpendicular virgin stress is obtained from:

$$\sigma_0 = \frac{\gamma H}{2} [(1+K) + (1-K) \cos 2\alpha] \quad \text{Eq 14}$$

where,  $\gamma$  = unit weight of the rock mass

K = ratio of the horizontal to vertical stress.

In Equation 13 the term  $(\chi \sin \alpha/2H)$  takes into account the variation in the virgin perpendicular stress on either side of the stope centre line. Unless the stope span is very large the term is not significant and Equation 13 can be simplified to:

$$C = \frac{4(1-\nu^2)}{E} \sigma_0 \sqrt{s^2 - \chi^2} \quad \text{Eq 15}$$

which is also the equation for a horizontal stope. Integrating Equation 15, with respect to  $(\chi)$ , gives the volumetric convergence per unit length along the stope:

$$Vc = \frac{2\pi(1-\nu^2)}{E} \sigma_0 s^2 \quad \text{Eq 16}$$

and from Equation 10 the change in potential energy is:

$$Wt = \frac{2\pi(1-\nu^2)}{E} \sigma_0^2 s^2 \quad \text{Eq 17}$$

The stored strain energy ( $U_m$ ) in the rock to be removed is relatively easy to calculate. For a perfectly elastic material the stored strain energy is:

$$U_m = \frac{1}{2E} [\sigma_1^2 + \sigma_2^2 + \sigma_3^2 - 2\nu(\sigma_1\sigma_2 + \sigma_2\sigma_3 + \sigma_3\sigma_1)] \quad \text{Eq 18}$$

where,  $U_m$  = stored strain energy per unit volume

$\sigma_1, \sigma_2, \sigma_3$  = principal stresses.

Again for tabular deposits the perpendicular stress ( $\sigma_p$ ) usually dominates and the stored strain energy can be approximated by:

$$U_m = \frac{\sigma_p^2(1-\nu^2)}{2E} \quad \text{Eq 19}$$

Returning to the example of an isolated thin stope, the perpendicular stress profile into the abutment can be expressed by:

$$\sigma_p = \frac{\chi\sigma_0}{\sqrt{\chi^2-s^2}} \quad (\chi \geq s) \quad \text{Eq 20}$$

and,

$$U_m = \frac{\sigma_0^2(1-\nu^2)\chi^2}{2E(\chi^2-s^2)} \quad \text{Eq 21}$$

Equation 20 predicts infinite stress at the edge of the abutment ( $\chi=s$ ) which is unrealistic, also Equation 21 is in a form difficult to integrate. However, an engineering approach can be used by dividing the abutment into a series of unit slices and calculating the average stress on each slice. The stored strain energies are summed for those slices to be removed in the next mining step.

Having calculated the change in potential energy ( $W_t$ ) by Equation 17, and the stored strain energy ( $U_m$ ) in the material to be removed in the next mining step by Equation 21, the other energy components ( $U_c$ ,  $W_r$ ,  $W_k$ ) can be calculated from Equations 4, 6 and 7.

#### INCREMENTAL VERSUS BULK MINING

As indicated in Equation 6 half the change in potential energy has to be released. How this energy is released, either as stored strain energy ( $U_m$ ) or seismic energy ( $W_k$ ), depends on the number and size of the mining steps used to achieve the final shape of the opening. This can be demonstrated by the simple example of a circular tunnel or shaft subjected to a hydrostatic stress ( $p$ ), for which a closed-form solution exists (Salamon, 1974).

The ratios ( $W_k/W_r$ ) and ( $U_m/W_r$ ) can be expressed by:

$$\frac{W_k}{W_r} = \frac{(1 - a^2/c^2)}{2(1-\nu)} \quad \text{Eq 22}$$

and, 
$$\frac{U_m}{W_r} = \frac{(1 - 2\nu + a^2/c^2)}{2(1-\nu)} \quad \text{Eq 23}$$

when the radius of the tunnel is enlarged from (a) to (c). Figure 3 shows how the energy is released as the tunnel is increased in radius to its final size. If the tunnel is created instantaneously (i.e., one mining step) then 62.5% of the released energy would be in the form of seismic energy and 37.5% as stored strain energy. However, if the radius was increased in 64 equal increments only 3.4% of the released energy is seismic energy and 96.6% as stored strain energy.

In Canadian hard rock mines there is an increasing tendency to the use of bulk mining techniques, wherever possible, due to the economics of scale. Figure 4 shows a typical layout of a blasthole stope in a vertical orebody. A 3 m high overcut and undercut are developed first, then the intervening orebody (26 m) is removed with large hole blasting techniques. The pre-mining horizontal and vertical stresses are taken as 50 MPa and 25 MPa, respectively, with the rock mass having an elastic modulus of 70 GPa and a Poisson's ratio of 0.2. A boundary element model was used to calculate the energy components which are listed in Table 1.

Table 1 - Energy components in a blasthole stope in (MJ/m in length)

Mining Stage	$\Delta W_t$	$\Delta U_m$	$\Delta U_c$	$\Delta W_r$	$\Delta W_k$	$\Delta W_k/\Delta W_r$
Overcut and undercut	3.2	0.6	2.2	1.6	1.0	62%
Blasthole	52.8	2.9	29.8	26.9	24.0	89%

These results indicate that when the blasthole section is mined a significant amount (about 90%) of the released energy is in the form of seismic energy.



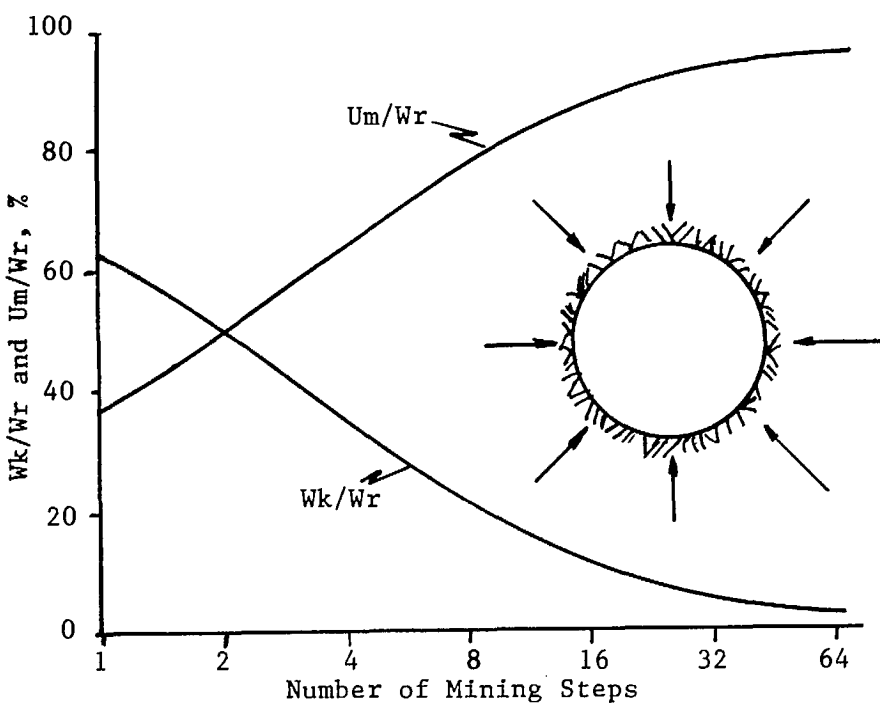


Fig. 3 - Variation in how energy is released with number of mining steps (after Salamon 1983).

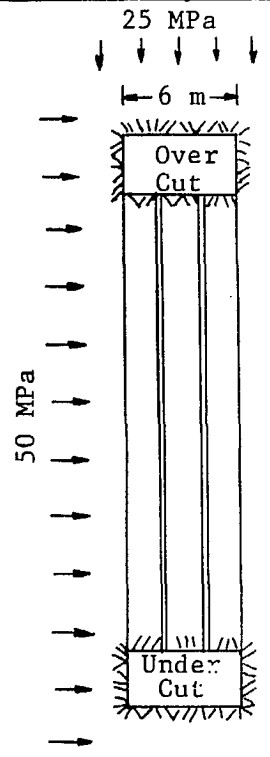


Fig. 4 - Blasthole stoping.

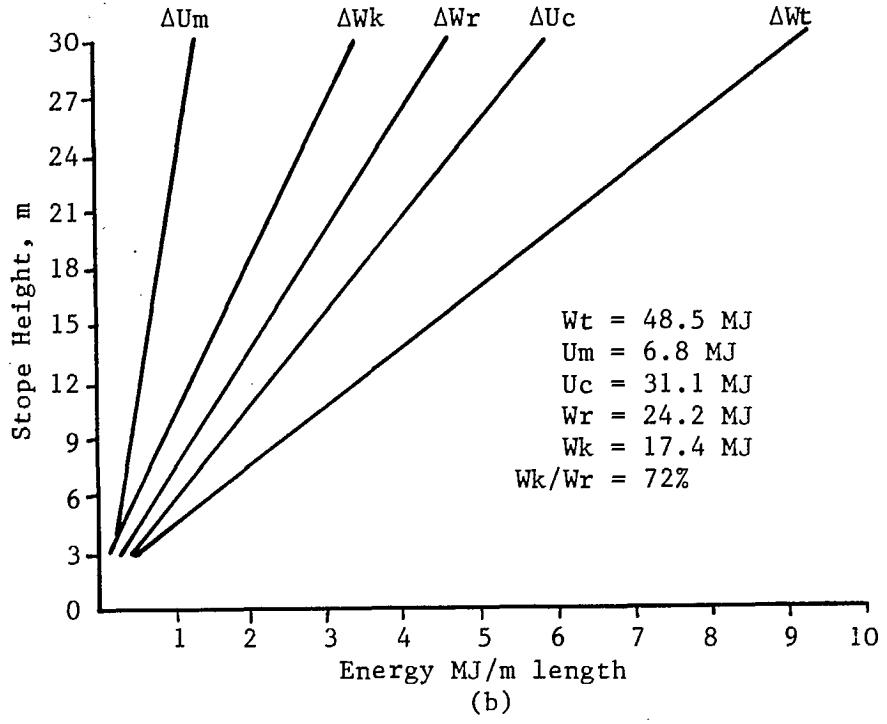
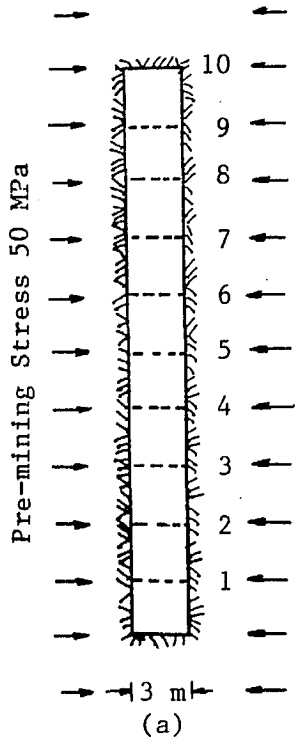


Fig. 5 - Energy components per cut during mining of a vertical stope.

Figure 5(a) shows a vertical unsupported stope which is mined upwards in 10 incremental cuts. The stope is 3 m wide and each cut is 3 m high. Only the pre-mining perpendicular stress of 50 MPa is used in this example, together with Equations 17 and 21. The incremental change in potential energy ( $\Delta W_k$ ) for each cut is obtained by subtracting the total change in potential energy of the previous cut from the present cut. The rock in the top abutment was divided into three horizontal 1 m slices to calculate the stored strain energy removed in the next cut.

Figure 5(b) shows the change in all energy components for each cut. Except for the first cut (not a good representation of a thin slit), there is a linear increase in all energy components as the stope progresses upwards. The total energy changes after 10 cuts are given at the bottom of Figure 5(b). Although the method of extraction could be classified as incremental, about 72% of the released energy is still in the form of seismic energy, even for these elastic conditions.

Suppose on the 10th cut in Figure 5(a) that three incremental slices are taken. This would more closely resemble horizontal drilling and breasting operations employed at many mines. In this case the boundary element model was used, because of the infinite stress at the face assumption in Equation 20. The results are presented in Table 2.

Table 2 - Energy components for three 1 m slices on the last cut  
(in MJ/m in length)

Slice	$\Delta W_t$	$\Delta U_m$	$\Delta U_c$	$\Delta W_r$	$\Delta W_k$	$\Delta W_k/\Delta W_r$
1	2.52	0.52	1.78	1.26	0.74	59%
2	2.61	0.54	1.84	1.30	0.77	59%
3	2.69	0.56	1.90	1.35	0.79	59%

By reducing the mining enlargement from 3 to 1 m reduces the seismic efficiency from 72% to 59%. However, this is still a long way from a seismic

efficiency approaching zero (i.e.,  $W_k = 0$ ). For this to happen the mining steps would have to be infinitesimally small, and probably equivalent to tunnel boring operations.

Theoretically, the seismic energy release in all these examples should occur within a fraction of a second following the blast. In practice it appears that the rock mass takes a longer time to adjust to the new stress regime. In a number of Canadian mines, rockbursts occur within a few seconds to hours after blasting. However, the longer the time interval the more probable that the cause of the rockburst is a breakdown of the rock mass rather than a purely elastic reaction.

#### TYPES OF ROCKBURSTS

The previous sections have dealt with the elastic reactions of the rock mass to mining. However, in most cases rockbursts are caused by the non-elastic rock behaviour during the failure process. Salamon (1983) has listed the pre-existing conditions necessary to initiate a rockburst. Part of the rock mass must be at the point of unstable equilibrium because either:

- a) changing stresses are driving a volume of rock to sudden failure;
- b) a system of pillars is approaching a state of imminent collapse;
- c) geological weakness planes are on the point of slipping.

These three categories can be conveniently labelled: strain, pillar, and fault-slip bursts, which are familiar terminology in mining.

Another condition is, that a change in stress is required to trigger the rockburst. This can either be an increase or decrease in stress depending on the type of rockburst. To initiate seismic waves an appreciable stress change must accompany the rockburst. Finally, there must be a substantial amount of energy available to provide the source of the seismic energy. This reservoir of energy can either be stored strain energy in the surrounding rock

mass or a sudden change in potential energy.

One grey area in rockburst mechanics is the time element. From seismic records, rockbursts occur instantaneously or in a matter of milli-seconds. It is not known whether the failure process will be violent if it is over seconds or even fractions of a second.

#### STRAIN BURSTS

Strain bursts are caused by high stress concentrations, at the edge of mine openings, which exceed the strength of the rock. Events can range from small slivers of rock being ejected from the walls to collapse of a complete wall as it tries to achieve a more stable shape. These types of rockbursts are normally associated with development drifts including shafts.

Originally, it was thought that the source of the liberated energy was the stored strain energy in the rock that had failed. This concept changed in the 1960's with the advent of stiff testing machines.

The mechanical equivalent of a compression testing machine is a mass resting on a spring in contact with a rock specimen as shown in Figure 6(a). As the mass is increased, energy is stored in both the rock specimen and spring. After the rock fails the load has to be reduced on both the failed rock specimen and the spring, and they will have different unloading curves. The gradient of the spring's unloading curve is called the spring constant ( $k$ ). Figure 6(b) shows the load-displacement with a relatively soft spring (i.e., low  $k$  value). After failure, the load the spring applies to the specimen is greater than it can withstand and failure will be sudden and violent. The area between the spring and specimen unloading curves represent the energy that has to be released seismically ( $Wk$ ). Figure 6(c) shows the same load-displacement curve for the specimen, but this time with a stiff spring (i.e., high  $k$  value). In this case, after failure, the load applied by the spring is less than what the specimen can withstand and the failure

process will be gradual and non-violent with no excess energy being released seismically.

The area under the specimen load-displacement curve is made up of two components: the stored strain energy ( $U_m$ ) of the specimen at its peak strength and part of the energy ( $U_s$ ) that was stored in the spring. These two components represent the energy ( $U_f = U_m + U_s$ ) consumed in the fracturing process. Consequently, the violence of rock failure is a property of the testing machine. The concept of loading and pillar stiffness is explored further under pillar bursts.

In some special cases part of the stored strain energy has to be released seismically. This occurs when a rock under triaxial stress conditions is suddenly reduced to a biaxial or uniaxial stress condition. The amount of energy stored in a rock under triaxial conditions was given in Equation 18. When mining an opening, one stress (say  $\sigma_3$ ) is reduced to zero. Assuming the other stresses remain constant the reduction in stored strain energy ( $\Delta U_m$ ) is:

$$\Delta U_m = \frac{1}{2E} [\sigma_3^2 - 2\nu(\sigma_2\sigma_3 + \sigma_3\sigma_1)] \quad \text{Eq 24}$$

Even more stored strain energy could be released if the rock, under triaxial stress, was just below its compressive strength. Figure 7(a) shows a specimen under triaxial stress in a testing machine, with a vertical stress ( $\sigma_v$ ). If the lateral stresses are suddenly reduced to zero, the maximum uniaxial compressive stress the specimen can withstand is ( $\sigma_u$ ) and ( $\sigma_u < \sigma_v$ ). As shown in Figure 7(b) the specimen will fail along its unloading curve, whereas the testing machine will unload, from the higher stress ( $\sigma_v$ ) along its unloading curve of gradient ( $k$ ). Again the area between these two unloading curves represents the energy that is released seismically ( $W_k$ ). The area identified at ( $\Delta U_m$ ) in Figure 7(a) is that proportion of the seismic energy

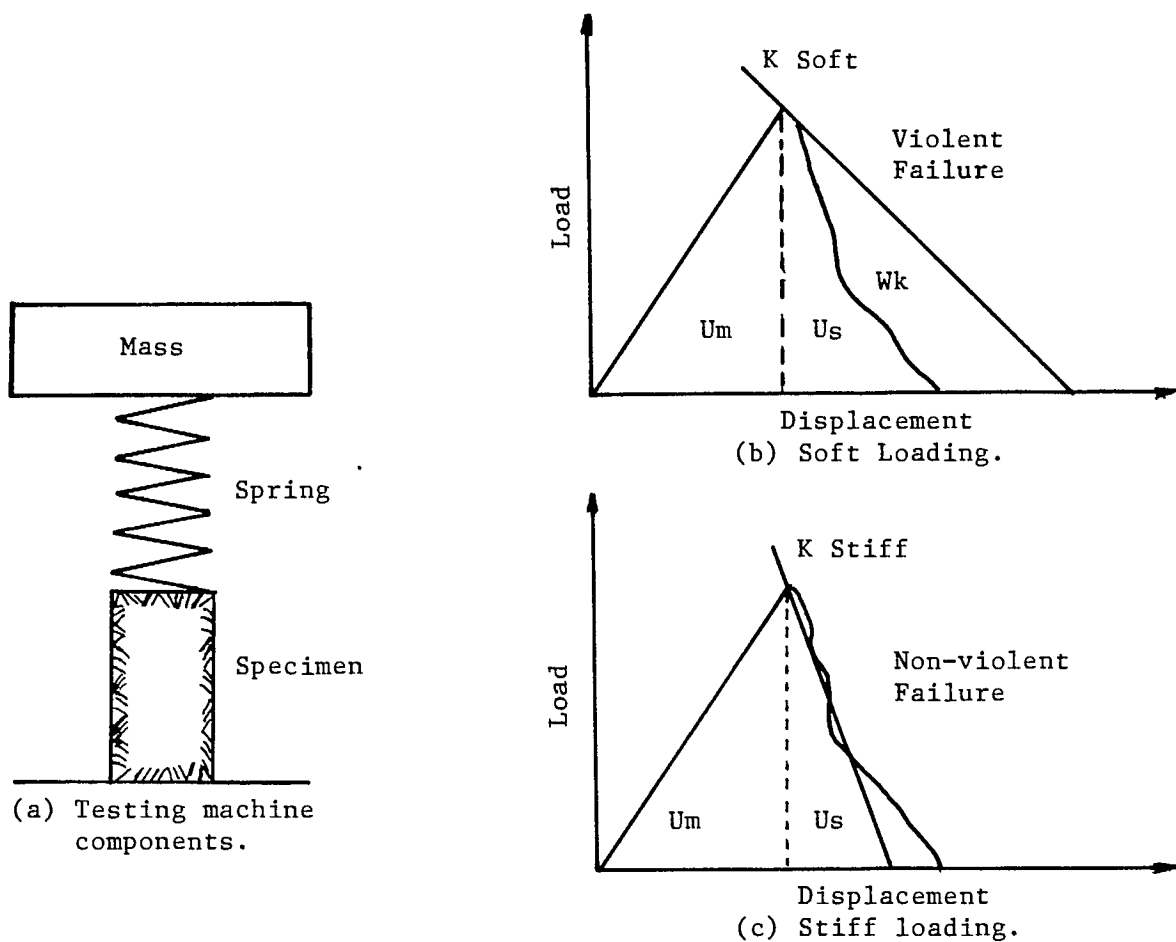


Fig. 6 - Violent and non-violent failure in soft and stiff testing machines.

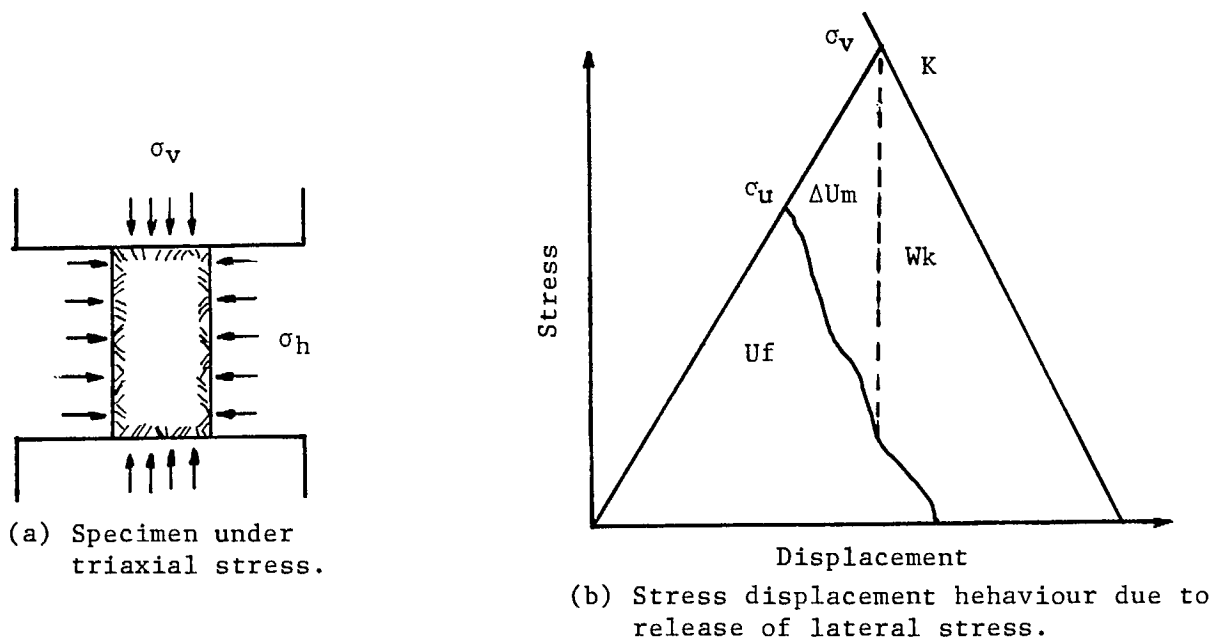


Fig. 7 - Release of stored strain energy due to loss of confinement.

which was originally stored as strain energy in the rock. In addition, the stored strain energy associated with the lateral stresses would also be released.

Strain bursts often occur when a drift is driven through a contact between a brittle and relatively soft rock. Damage is normally confined to the brittle side of the contact. Previously it was thought that the brittle rock, with a higher compressive strength and elastic modulus, would contain more stored strain energy. This is not necessarily the case as illustrated in Figure 8. Brittle rocks tend to have steeper unloading curves than soft rocks. In Figure 8, the area under both brittle and soft load-displacement curves are roughly the same, hence both rocks consume the same stored strain energy in the fracturing process. Again, the stiffness of the loading system ( $k$ ) is less than that of the brittle rock and greater than the soft rock. Hence, the former fails violently and the latter non-violently, in this example.

Another mechanism that could be in operation is slippage along the contact. For the simple example of a circular tunnel excavated in a hydrostatic stress field ( $p$ ) the radial displacement ( $u$ ) of the circumference is given by:

$$u = \frac{rp}{E} (1 + \nu) \quad \text{Eq 25}$$

where,  $r$  = radius of opening.

If the elastic modulus of the soft rock is half that of the brittle rock then the radial displacement is double for the soft rock. This would generate shear stresses along the contact with a chance of slippage.

Figure 9 shows a rectangular shaft which was subjected to a very high horizontal stress (70 MPa) across its short axis. At a depth of 1000 m one of the short walls burst in a semi-circular shape, at a contact between a brittle

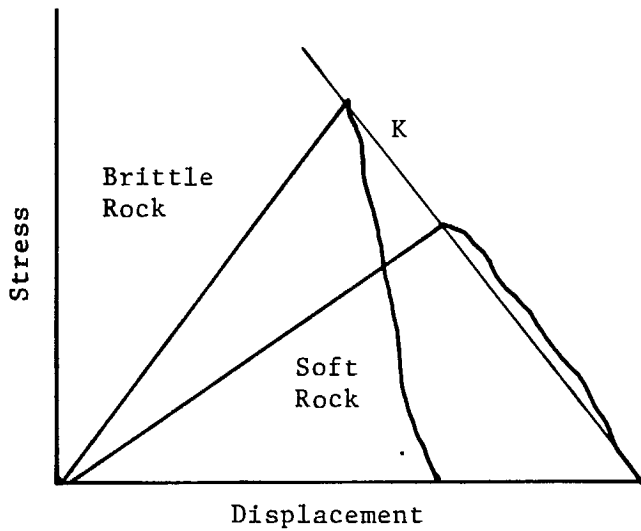


Fig. 8 - Stress-displacement characteristics of brittle and soft rocks.

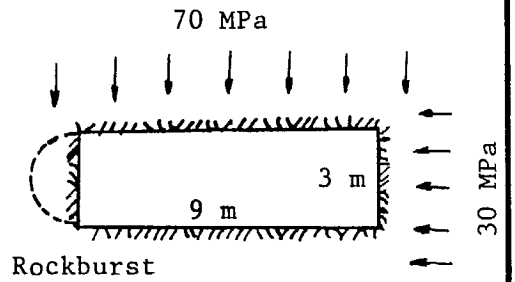


Fig. 9 - Rockburst in a rectangular shaft.

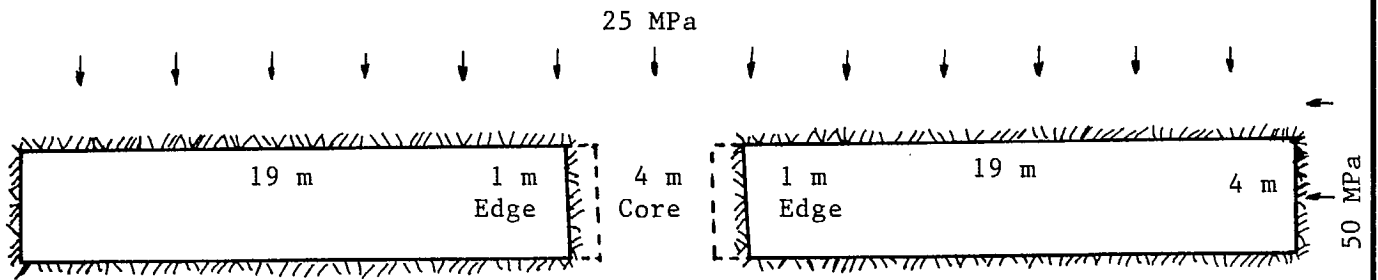


Fig. 10 - Stope and pillar model with two stages of pillar failure.

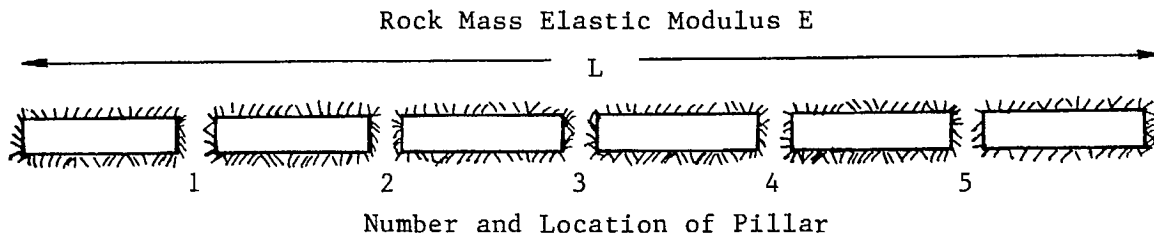


Fig. 11 - Factors affecting loading stiffness.



quartzite and a soft dyke. A boundary element model was run to determine the energy component due to the wall going from a straight to semi-circular shape. These components are listed in Table 3.

Table 3 - Energy components for a burst in a shaft (in MJ/m in length)

$\Delta W_t$	$\Delta U_m$	$\Delta U_c$	$\Delta W_r$	$\Delta W_k$	$\Delta W_k/\Delta W_r$
2.46	0.50	1.73	1.23	0.73	59%

Somewhat surprisingly, 59% of the released energy is seismic energy.

It appears that for strain bursts, energy can be released from a number of sources. If the rock goes from a triaxial to biaxial or uniaxial stress condition, some of the stored strain energy is released as seismic energy. Instantaneous failure of this rock will enlarge the opening and seismic energy will be released due to the elastic reactions of the rock mass (i.e., as in the example of the rectangular shaft). Finally, if brittle and soft rocks are present, then minor slippage could occur along the contact.

#### PILLAR BURSTS

Severe rockbursts, involving thousands of tonnes, have been caused by the complete collapse of support pillars. In some cases the collapse of one pillar can overstress adjacent pillars and a chain-type reaction ensues. In recent times, the most significant chain reaction occurred in an old stope-and-pillar area of Quirke Mine in Elliot Lake. Over a six month period there were over 140 rockbursts of magnitude 1.5 to 3.0  $M_N$ . Significant pillar bursts have also occurred in steeply-dipping vein-type orebodies at Red Lake and Kirkland Lake. These normally occur when sill/crown pillars of shrinkage or cut-and-fill stopes reach a critical size.

The source of the liberated seismic energy can be demonstrated by the simple example of two stopes separated by a pillar as shown in Figure 10. Two

cases are examined: the edge of the pillar failing, followed by the central core. In both cases it is assumed that the stress on the failed portion reduces immediately to zero (i.e., a vertical unloading line from peak strength). The boundary element model was used to calculate the energy components for the two stages of failure, which are given in Table 4.

Table 4 - Energy components for partial and complete pillar failure (in MJ/m in length).

Failure Stage	$\Delta Wt$	$\Delta U_m$	$\Delta U_c$	$\Delta W_r$	$\Delta W_k$	$\Delta W_k/\Delta W_r$
Edges	1.62	0.30	1.11	0.81	0.51	63%
Core	10.73	0.93	6.29	5.36	4.44	83%

These results indicate a seismic efficiency ( $\Delta W_k/\Delta W_r$ ) of 63% during failure of the pillar edges, which increases to 83% when the core fails. It appears that one of the characteristics of pillar bursts is that a very high proportion of the released energy ( $W_r$ ) is seismic energy ( $W_k$ ). The source of this liberated energy is the large change in potential energy ( $W_t$ ) when the pillar fails. Equation 17 indicates that the change in potential energy is proportional to the square of the stope span. In this case, when the pillar core fails, the stope span more than doubles, hence the change in potential energy more than quadruples.

Whether a pillar fails violently or not depends on the stiffness of the loading system compared to that of the pillar, as explained in an elementary way in Figure 6. If the stiffness of the loading system is ( $k$ ) (defined as always positive) and that of the pillar is ( $\lambda$ ) then the condition for stability is:

$$k + \lambda > 0 \quad \text{Eq 26}$$

If the pillar is on its loading curve, ( $\lambda$ ) is positive and conditions are stable. It is only when the pillar exceeds its peak strength and its

unloading curve ( $\lambda$ ) is negative and exceeds the loading stiffness ( $k$ ) that instability occurs.

In underground mines the stiffness of the loading system is influenced by many factors as illustrated in Figure 11. The areal extent or span of the mine workings has a strong influence. As the span increases loading stiffness decreases and eventually approaches a dead-weight loading system (i.e.,  $k=0$ ). The elastic modulus of the rock mass controls the amount of movement towards the excavations. The size, number and location of the pillars influence loading stiffness. Also, pillars cannot be treated in isolation since the presence of one pillar influences the loading stiffness on all other pillars.

The concept of local mine stiffness was introduced by Starfield and Fairhurst (1968). Suppose in Figure 11, that one of the pillars is replaced by a hydraulic jack which exerts the same load as the original pillar. The local mine stiffness, at that location, would be the unloading curve for the jack as the pressure is released. It can be envisaged that each pillar in turn is replaced by a hydraulic jack, thus obtaining the profile of loading stiffness across the panel. For a systematic layout of stopes and pillars the results would show that the loading system has its lowest stiffness at the centre of the panel and its highest stiffness next to the abutments. It follows that if one pillar fails the loading stiffness on all the remaining pillars reduces.

A family of stress-displacement curves can be obtained by testing specimens in a compression testing machine, as shown in Figure 12. As either width/height ratio or confining stress increases the post-failure gradient (i.e., pillar stiffness  $\lambda$ ) becomes flatter. This indicates that slender pillars, with a low width/height ratio are more prone to bursting than squat pillars, since their unloading gradient has a high negative value. However, experience underground suggests the complete reverse; slender pillars tend to

yield and fail non-violently, whereas squat pillars fail violently. This apparent contradiction was resolved by Salamon (1970), in that loading and pillar stiffness cannot be treated in isolation, but must be considered in terms of all the pillars. Equation 26 only applies to testing single specimens in a press and its correct formulation is:

$$K + \Lambda > 0 \quad \text{Eq 27}$$

where (K) is the loading stiffness matrix on all the pillars and ( $\Lambda$ ) is the slope matrix for all the pillars. It can be seen that for a mixture of slender and squat pillars, the slender ones would fail first, as indicated in Figure 12. Their slope would become negative, but the squat pillars would still be on their loading curve with a positive slope and (K +  $\Lambda$ ) would still be greater than zero. With the slender pillars failing the loading stiffness would decrease and eventually, with increasing stress the squat pillars would fail violently.

This concept was demonstrated, in the laboratory, by loading multiple specimens at the same time, Swan (1985). As shown in Figure 13, a central aluminum pillar was surrounded by nine rock specimens of varying width/height ratio. Each specimen had its own load cell to measure its complete load-displacement history. Figure 14 shows the load-displacement curves for two of the specimens, of width/height ratios 0.5 and 1.0, as well as the central aluminum pillar. It was difficult to make each specimen the same height so their loading curves start at different displacements of the platen. By design the aluminum pillar was made slightly shorter so that the load capacity of the press was not used up compressing it.

The slender specimen failed first non-violently. Its slope became negative ( $\lambda = -3.2 \text{ MN/mm}$ ), but the remaining specimens plus the central pillar were still on their loading curves with positive slopes. The squatter specimen failed next, again non-violently, with a similar negative slope

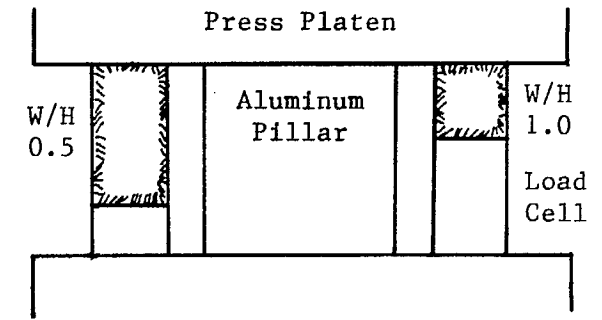
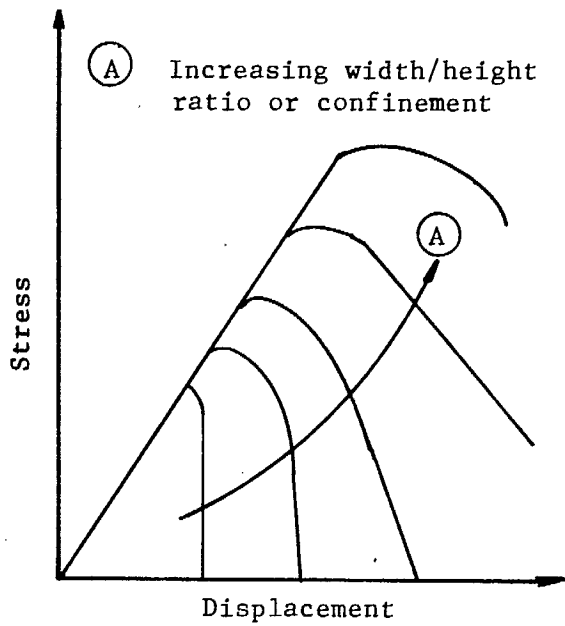


Fig. 13 - Multiple specimen testing.

Fig. 12 - Factors affecting the post-failure stiffness of pillars.

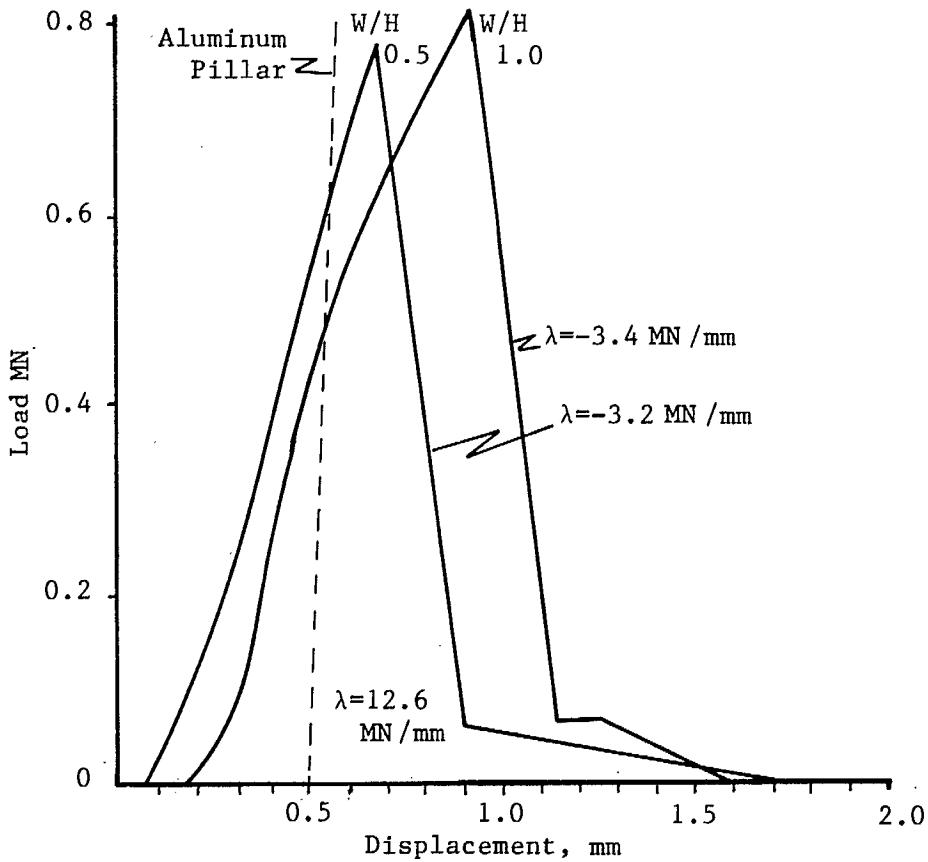


Fig. 14 - Load-displacement history of two specimens and aluminum pillar loaded simultaneously.

( $\lambda = -3.4 \text{ MN/mm}$ ). In all, six of the nine specimens failed non-violently at peak strengths ranging from 175 to 235 MPa. At this point the test was terminated due to tilting of the platen. Although, in this test, the loading stiffness of the testing machine is constant, it did show that the slope matrix ( $\Lambda$ ) for all the specimens including the central aluminum pillar controls whether the specimens fail violently or not.

In summary, it appears that pillar bursts are caused by a sudden change in potential energy as the hanging wall and footwall rapidly converge during the failure process. Whether a pillar fails violently or not depends on the post-failure stiffness of the pillar compared to the stiffness of the loading system. However, pillar and loading stiffness cannot be treated in isolation, but must be considered in regional terms involving whole stope-and-pillar panels and in some cases the whole mine.

#### FAULT-SLIP BURSTS

Slippage along a fault has long been recognized as the mechanism of an earthquake. Only recently has the same mechanism been recognized as the cause of some rockbursts in Canadian hardrock mines, especially those in Sudbury.

A simple mechanical model which demonstrates fault-slip mechanics is shown in Figure 15(a). A block under a normal stress ( $\sigma_n$ ) rests on a flat surface. A tangential stress ( $\tau$ ) is applied through an elastic spring (spring constant  $k$ ), to the edge of the block. After the normal stress is applied the frictional force between the block and the flat surface is ( $\mu_s \sigma_n$ ), where ( $\mu_s$ ) is the static coefficient of friction. The system is in stable equilibrium so long as:

$$\mu_s \sigma_n - \tau > 0 \quad \text{Eq 28}$$

Unstable equilibrium is achieved when:

$$\tau = \mu_s \sigma_n \quad \text{Eq 29}$$

Movement of the block will occur if there is a very small increase in

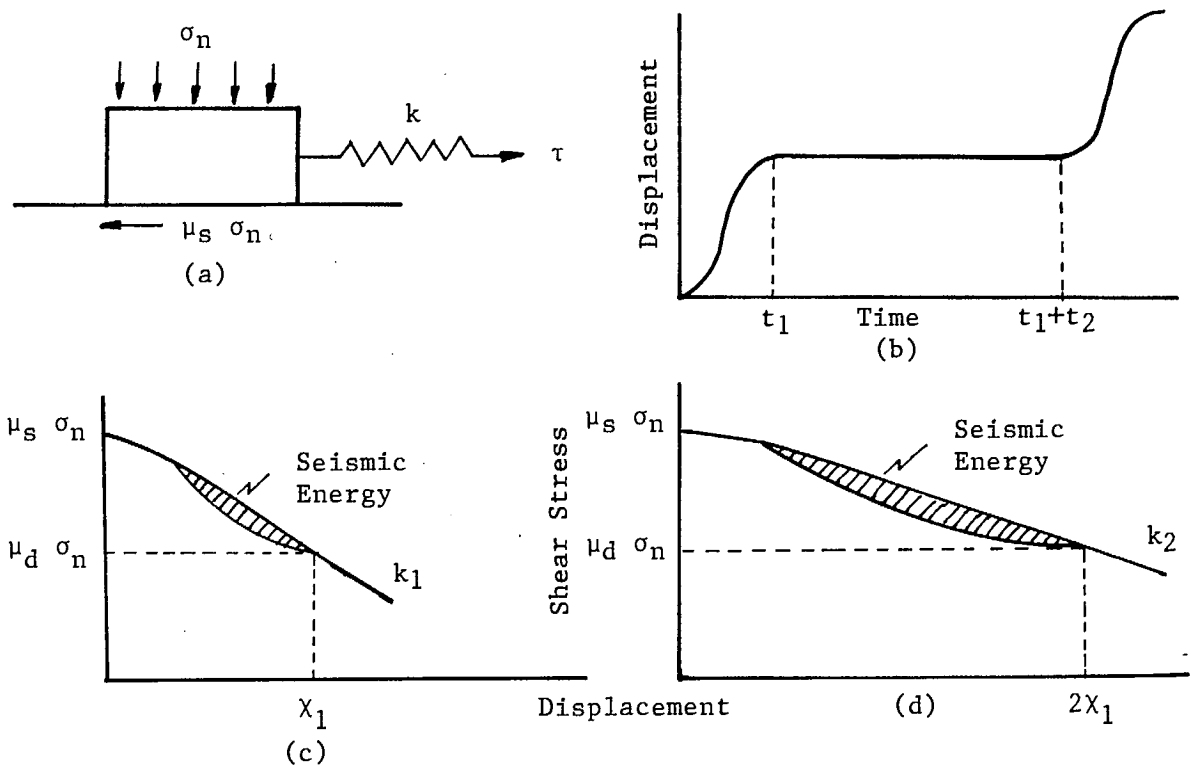


Fig. 15 - Displacement, time, shear stress history of fault-slip model.

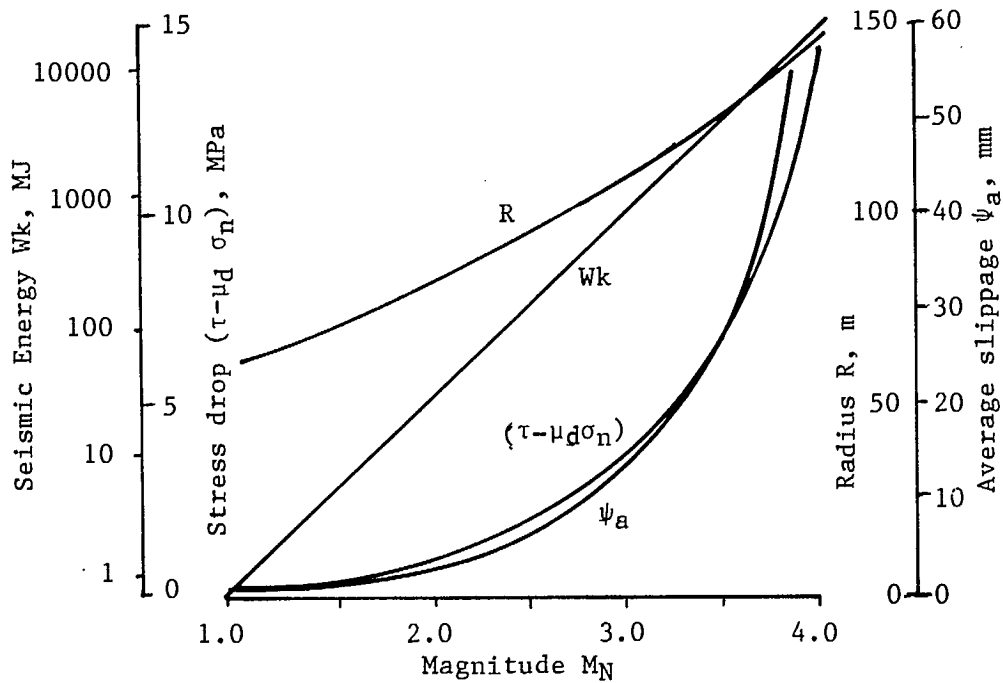


Fig. 16 - Estimation of fault-slip parameters.

( $\tau$ ) or a decrease in ( $\sigma_n$ ) or ( $\mu_s$ ). Once movement occurs the lower dynamic coefficient of friction ( $\mu_d$ ) comes into operation and an initial force of:

$$(\mu_s - \mu_d)\sigma_n$$

accelerates the block. Stable equilibrium is achieved when the shear stress reduces to:

$$\tau' = \mu_d \sigma_n \quad \text{Eq 30}$$

and the resultant stress drop is:

$$(\tau - \mu_d \sigma_n) \quad \text{Eq 31}$$

The dynamic history of the block movement is shown in Figure 15(b) (Jaeger and Cook, 1969). Here it is assumed that the free end of the spring moves at a constant velocity away from the block. Replacing the normal stress ( $\sigma_n$ ) by a force (N) pressing on a mass (M), then the displacement ( $\chi$ ) of the block with respect to time (t) is:

$$\chi = (\mu_s - \mu_d) \frac{N}{k} (1 - \cos \alpha t) \quad \text{Eq 32}$$

where  $\alpha^2 = k/M$ .

The block comes to rest at time ( $t_1$ ):

$$t_1 = 2\pi/\alpha \quad \text{Eq 33}$$

after a displacement ( $\chi_1$ ):

$$\chi_1 = 2 (\mu_s - \mu_d) \frac{N}{k} \quad \text{Eq 34}$$

If the end of the spring continues to move at a constant velocity then after an additional time ( $t_2$ ) the spring is recharged and the whole slippage cycle repeats itself.

Figure 15(c) shows the stress-displacement history of the block. Again, displacement starts when the shear stress equals ( $\mu_s \sigma_n$ ) and stops when it reduces to ( $\mu_d \sigma_n$ ). The curve of block displacement can be non-linear as illustrated, whereas the spring has a linear unloading curve of gradient ( $k_1$ ). The area between the two curves represents the energy that has to be



dissipated kinetically. This is analogous to the specimen and loading machine stiffness concepts discussed earlier. The total kinetic energy ( $W_k$ ) released can be expressed by:

$$W_k = \frac{N^2 \Pi}{2k\alpha} (\mu_s - \mu_d)^2 \quad \text{Eq 35}$$

Figure 15(d) shows the stress-displacement history if the spring constant is reduced by a half ( $k_2 = k_1/2$ ). In this case the displacement of the block is doubled (from Equation 34) and the area between the two curves is increased. This emphasizes the importance of the stiffness of the loading system on both the amount of slippage and seismic energy released in fault-slip rockbursts.

The mechanics of slippage on a fault with a circular area have been developed in rock mechanics by Salamon (1974), and in seismology by Brune (1970). Using Salamon's terminology, the drop in the shear stress is:

$$\tau - \mu_d \sigma_n$$

For a circular fault of radius ( $R$ ) in homogeneous isotropic ground, the tangential slip ( $\psi$ ), is given by:

$$\psi = \frac{4(1 - \nu)(\tau - \mu_d \sigma_n)(R^2 - r^2)^{1/2}}{\Pi G (1 - \nu/2)} \quad \text{Eq 36}$$

where,  $r$  = distance from centre

$\nu$  = Poisson's ratio

$G$  = modulus of rigidity (shear modulus).

The energy components can be expressed as follows:

$$\text{Potential Energy, } W_t = \frac{8(1 - \nu)R^3 \tau (\tau - \mu_d \sigma_n)}{3G(1 - \nu/2)} \quad \text{Eq 37}$$

$$\text{Released Energy, } W_r = \frac{4(1 - \nu)R^3 (\tau + \mu_d \sigma_n)(\tau - \mu_d \sigma_n)}{3G(1 - \nu/2)} \quad \text{Eq 38}$$

$$\text{Heat Energy, } W_h = \frac{8(1 - \nu)R^3 \mu_d \sigma_n (\tau - \mu_d \sigma_n)}{3G(1 - \nu/2)} \quad \text{Eq 39}$$

$$\text{Seismic Energy, } W_k = W_r - W_h = \frac{4(1 - \nu)R^3(\tau - \mu_d \sigma_n)^2}{3G(1 - \nu/2)} \quad \text{Eq 40}$$

The seismic efficiency can be calculated from these relationships:

$$W_k/W_r = \frac{\tau - \mu_d \sigma_n}{\tau + \mu_d \sigma_n} \quad \text{Eq 41}$$

Just before slip initiation the shear and frictional forces are in equilibrium:

$$\tau = \mu_s \sigma_n \quad \text{Eq 42}$$

Hence,

$$\frac{W_k}{W_r} = \frac{\mu_s - \mu_d}{\mu_s + \mu_d} \quad \text{Eq 43}$$

This analysis indicates that seismic efficiency is independent of depth, stress drop, fault dimensions or amount of slippage and is only dependent on the frictional properties of the fault. Typically the dynamic coefficient of friction is 90 to 95% of the static coefficient (Jaeger & Cook, 1969), giving seismic efficiencies of 5% to 2.5%. This is completely the reverse of the seismic efficiencies, of about 90%, encountered in pillar rockbursts.

In seismology the seismic moment ( $M_o$ ) is used to define the size and magnitude of an earthquake. Seismic moment is defined as the product of the average slip ( $\psi a$ ), shear modulus and area. For a circular fault:

$$M_o = \psi a G \Pi R^2 \quad \text{Eq 44}$$

From Equation 36:

$$\psi a = \frac{(1 - \nu)(\tau - \mu_d \sigma_n)R}{(1 - \nu/2)G} \quad \text{Eq 45}$$

and

$$M_o = \frac{\Pi(1 - \nu)(\tau - \mu_d \sigma_n)R^3}{(1 - \nu/2)} \quad \text{Eq 46}$$

This equation can be compared with one from the circular fault model developed by Brune (1970):

$$M_o = \frac{16}{7}(\tau - \mu_d \sigma_n)R^3 \quad \text{Eq 47}$$

For a typical Poisson's ratio of 0.2, Equation 46 gives a seismic

moment 22% greater than Equation 47.

Using some empirical relationships, developed in seismology, it is possible to estimate the parameters (seismic energy, stress drop, radius and average slippage) involved with fault-slip type rockbursts. For the Canadian Shield, Hasegawa (1983) has shown that the relationship between seismic moment and magnitude can be expressed by:

$$\log M_o = 4.32 + 0.94 M_N \quad \text{Eq 48}$$

where,  $M_N$  is the magnitude scale developed by Nuttli (1973) for eastern North America. The relationship between seismic energy and magnitude is:

$$\log W_k = 1.5 M_N - 1.65 \quad \text{Eq 49}$$

From Equations 40 and 46:

$$\frac{W_k}{M_o} = \frac{4(\tau - \mu_d \sigma_n)}{3\pi G} \quad \text{Eq 50}$$

Using a typical shear modulus of 30,000 MPa and converting to a log relationship:

$$\log W_k = \log M_o + \log (\tau - \mu_d \sigma_n) - 4.85 \quad \text{Eq 51}$$

Equations 48 and 49 can now be substituted into Equation 51 to give:

$$\log(\tau - \mu_d \sigma_n) = 0.56 M_N - 1.12 \quad \text{Eq 52}$$

Estimates can now be made for the stress drop ( $\tau - \mu_d \sigma_n$ ) from Equation 52, liberated seismic energy ( $W_k$ ) from Equation 49, fault radius ( $R$ ) from Equation 40, and average slippage ( $\psi a$ ) from Equation 45. These relationships are shown in Figure 16 for rockburst magnitudes 1.0 to 4.0  $M_N$ .

These results give only a rough estimate since the empirical relationships 48 and 49 are logarithmic and prone to large errors. However, the analysis does indicate that only minor stress drops and slippage are required to produce significant rockbursts. For instance, a rockburst of magnitude 3.0  $M_N$  would result from a stress drop of 3.5 MPa with an average slippage of 12 mm over a radius of 100 m.

In most mining operations the faults, on which slippage is occurring, intersect the mine openings. A full circular fault model may not be applicable in these cases and a semi-circular or quadrant model may be more appropriate. In some cases the aftershock pattern from microseismic monitoring systems gives a good indication of the areal extent over which slippage occurred.

In most cases, the damage caused by fault-slip rockbursts in Ontario mines is minimal. There is one example of a 2.2  $M_N$  magnitude rockburst at the Falconbridge Mine near Sudbury where no damage was found, although 10 to 20 mm of slippage could be observed on the fault. Normally what damage is observed is away from the fault where the radiated seismic energy has triggered a critically loaded structure. In one case a 3.4  $M_N$  fault-slip rockburst caused a backfill mat to collapse in an undercut-and-fill stope some 20 m away.

#### REFERENCES

- Brune, J.N. (1970), Tectonic stress and the spectra of seismic shear waves from earthquakes; *J. Geophys. Res.*, vol. 75, pp. 4997-5009. Correction: *J. Geophys. Res.* vol. 76, (1971), p. 5002.
- Cook, N.G.W. (1967), Design of underground excavations; 8th U.S. Rock Mech. Symp., Minnesota, pp. 167-193.
- Hasegawa, H.S. (1983), Lg spectra of local earthquakes recorded by the Eastern Canada telemetered network and spectral scaling; *Bull. Seis. Soc. Am.*, vol. 73, No. 4, pp. 1041-1061.
- Hodgson, K. and Joughin, N.C. (1967), The relationship between energy release rate, damage and seismicity in deep mines; 8th U.S. Rock Mech. Symp., Minnesota, pp. 194-209.
- Nuttli, O.W. (1973), Seismic wave attenuation and magnitude relations for eastern North America, *J. Geophys. Res.*, vol. 78, pp. 876-885.

- Ortlepp, W.D. (1983), The mechanism and control of rockbursts; Chapter 12: Rock Mechanics in Mining Practice, S. Budavari (Editor), S. Afr. Inst. Min. Met., Mono Series No. 5, pp. 257-281.
- Salamon, M.D.G. (1968), Two-dimensional treatment of problems arising from mining tabular deposits in isotropic or transversely isotropic ground; Int. J. Rock Mech. Min. Sci., vol. 5, pp. 159-185.
- Salamon, M.D.G. (1970), Stability, instability and design of pillar workings; Int. J. Rock Mech. Min. Sci., vol. 7, pp. 613-631.
- Salamon, M.D.G. (1974), Rock mechanics of underground excavations; Proc. 3rd Congr. Int. Soc. Rock Mech., Denver, Colorado, vol. 1, Part B, pp 951-1099.
- Salamon, M.D.G. (1983), Rockburst hazard and the fight for its alleviation in South African gold mines; Rockbursts: Prediction and Control, IMM, London, pp 11-36.
- Salamon, M.D.G. (1984), Energy considerations in rock mechanics: fundamental results, J. S. Afr. Inst. Min. Met. vol. 84, No. 8, pp. 233-246.
- Starfield, A.M. and Fairhurst, C. (1968), How high-speed computers can advance design of practical mine pillar systems; Eng. & Min. J., vol. 169, pp. 78-84.
- Swan, G. (1985), Multiple pillar compression failure in brittle rock, Division Report MPR/MRL 85-103(TR), CANMET, Energy, Mines and Resources Canada.

## APPENDIX

EXENBRAY: A computer program for determining the energy released from underground excavations based on Salamon's energy formulation and utilizing the fictitious force indirect boundary element method of Bray.

Developed by: Department of Civil Engineering,  
University of Toronto.

For: CANMET, Energy, Mines and Resources Canada.

ENERGY FORMULATION OF SALAMON

In the past two decades, numerous workers have studied the importance of energy changes that take place in the process of excavating underground openings. The work of Salamon (1984) contains the most complete and rigorous analysis of this problem which is summarized in the synopsis of his paper, repeated in part below:

"If a transition from one equilibrium state to another occurs during the course of mining, energy transfer takes place in the rock mass, which is assumed to be an elastic continuum. The energy components are defined as follows: the work done by external and body forces,  $W_t$ ; the increase in stored energy in the mass,  $U_c$ ; the strain energy in the rock mined during the transition,  $U_m$ ; the work done on mine support or backfill,  $W_s$ ; and the released energy  $W_r$ . The energy balance is defined as  $(W_t + U_m) - (U_c + W_s) = W_r > 0$ , where the first set of components in parentheses represents the sources of energy, while that of the second corresponds to the known modes of energy expenditure and the component on the right is the unaccounted-for energy surplus, which must be released and dissipated in some form. The inequality  $W_r \geq U_m > 0$  applies."

Considering the problem of the energy changes resulting from changes from a geometry in State I to State II as shown in Figure A-1, Salamon shows that for an unsupported cavity in a weightless medium the energy balance in moving from State I to State II can be determined from the evaluation of two components of energy.

These are  $U^{(ii)}$ , the strain energy stored in volume  $V$  if the induced stresses were to act on the originally unstrained body and  $U_m$ , the strain energy content, of  $V_m$  in State I. Adopting the convention that  $V_m$  is the volume of rock excavated in the transition from State I to State II, and  $S_m$  is the unexposed part of the boundary surface of  $V_m$ , Salamon showed that for this case:

$$U^{(ii)} = 1/2 \int_{S_m} T_i^{(p)} u_i^{(i)} dS \quad \text{Eq A-1}$$

and

$$U_m = 1/2 \int_{S_m} T_i^{(p)} u_i^{(p)} dS \quad \text{Eq A-2}$$

where, superscript  $p$  stands for 'primitive' or 'of earlier state'

superscript  $i$  denotes components induced by additional mining

subscript  $i$  denotes components of the vector.

Thus,  $T_i$  is the stress or traction vector acting on a surface, and  $u_i$  is the associated displacement.

Equations A-1 and A-2 lead to:

$$U_c = U^{(ii)} + 2 U_m$$

$$W_t = 2[U^{(ii)} + U_m]$$

$$W_s = 0$$

$$W_r = U^{(ii)} + U_m = W_t/2 \quad \text{Eq A-3}$$

$$W_k = U^{(ii)}$$

Thus, all the necessary energy components in moving from State I to State I for a weightless medium may be determined from the values of  $U^{(ii)}$  and  $U_m$ .

EXENBRAY PROGRAM

The EXENBRAY Program was developed in the Department of Civil Engineering, University of Toronto. It is based on Bray's (1976) Fictitious Force Boundary Element Program, BEM 2D, Version 2.2.

The function of EXENBRAY is to evaluate the energy changes associated with multiple stages of underground excavation in a rock mass. The new excavation may completely enclose the previous excavations, extend boundaries of existing openings and include the removal of rock between adjacent openings.

The program has been developed in a completely user-friendly manner. The two means of data input are an interactive mode or through the use of data files. Data input in the interactive mode is also stored in a data file for future reference. At the end of each analysis, a statement of the energy changes with each stage of excavation is output to the screen. Hard copy comprises the complete output of the analysis which is stored in an output file. Thus the program EXENBRAY can also function in the original mode of Bray's program version 2.2.

The program (now called version 1.1) is written, wherever possible, in Fortran 77. This was done with the view to making the new program compatible with the version 2.2 program. Changes to the version 2.2 program, in making the new EXENBRAY program, are made in lower case. The program flow chart is shown in Figure A-2 and was implemented at the Engineering Computing facility, University of Toronto on a VAX 11/780 computer operating under the UNIX operating system.

Subsequently, the program has been slightly modified to run on an IBM-PC. The example input/output and program listing, given later, are the IBM-PC version. The maximum number of elements depends on the memory size and hard disk availability for compiling (e.g., a 640 K IBM-PC with hard disk can use



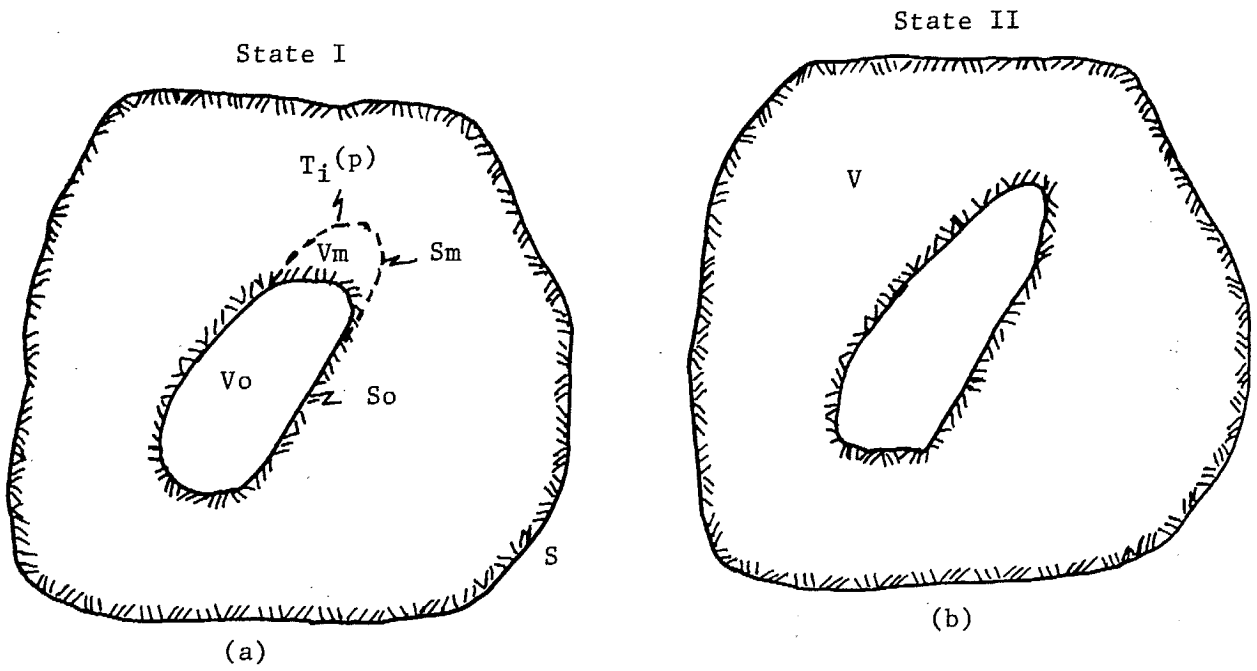


Fig. A-1 - Mining configuration and notations for State I and State II.

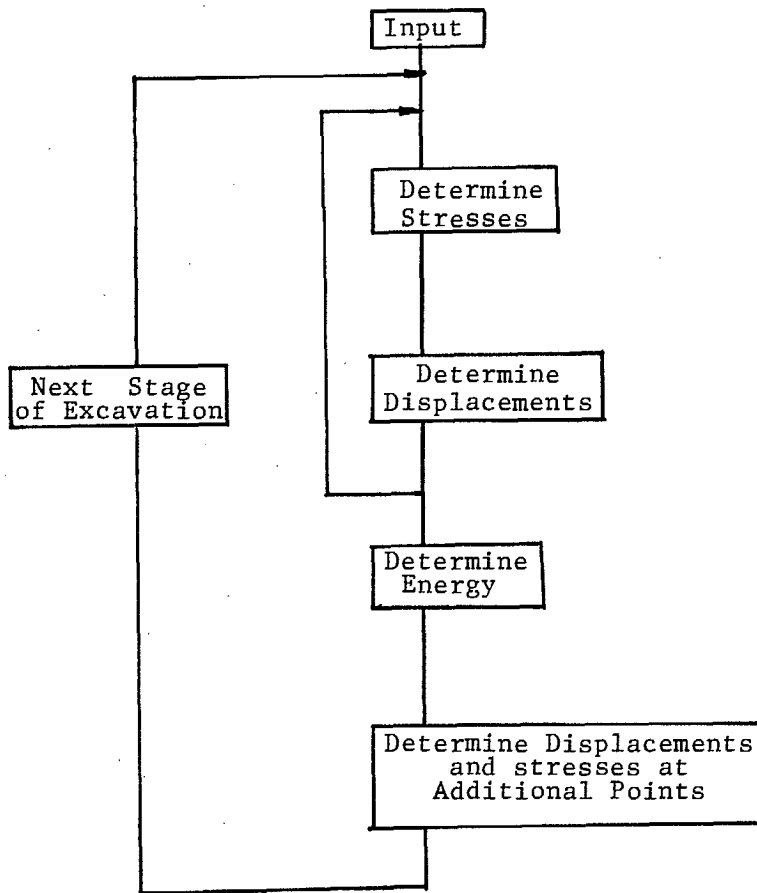


Fig. A-2 - Program flow chart.

up to 130 elements).

### PROGRAM FORMULATION

In order to determine the energy components given in Equations A-1 and A-2, it is necessary to determine the specified displacements and tractions, namely,  $T_i^{(p)}$ ,  $u_i^{(p)}$  and  $u_i^{(i)}$ . The tractions ( $T_i^{(p)}$ ) correspond to the tractions on the imaginary, unexcavated Stage II boundary when the excavation is at Stage I as shown in Figure A-1. These tractions can be determined directly from Bray's original computer code.

Displacements  $u_i^{(i)}$  correspond to the displacements  $u_i$  of points on the Stage II boundary as the excavation proceeds from the Stage I cavity to the Stage II cavity. If we denote the displacement of an arbitrary point on the Stage II boundary due to the Stage I excavation as  $u_{i,II,I}$ , and the displacement of the same point due to the Stage II excavation as  $u_{i,II,II}$ , then  $u_i^{(i)} = (u_{i,II,II} - u_{i,II,I})$ .

Both displacements  $u_{i,II,II}$  and  $u_{i,II,I}$  can be determined by means of Bray's program.

Evaluation of  $U_m$  requires a knowledge of  $u_i^{(p)}$ . It was noted that Bray's program calculates the displacements which are induced by the excavation. Thus, the free field displacements must be added to those induced by the excavation in order to find  $u_i^{(p)}$ , giving:

$$u_i^{(p)} = u_{i,II,I} + u_{i,\text{free field}}$$

The free field displacements are evaluated for the stressed medium without an opening. The free field deformations may be determined with respect to an arbitrary origin since, in the evaluation of the energy integrals, rigid body displacements of a body in static equilibrium causes no work to be done.

## EXENBRAY USERS MANUAL

INTRODUCTION

EXENBRAY is a FORTRAN computer program for determining the energy released and the stress and displacement distributions in plane strain condition around an excavation in an infinite medium. This program is modified from the computer program BEM 2D, Version 2.2, of Bray (1976).

For the analysis of the energy released due to underground excavations in an elastic medium, the Boundary Element method does offer significant advantages over the Finite Element method. The time and effort to prepare the input data are dramatically reduced.

The program EXENBRAY is designed to determine both the energy released and the stress distribution in problems which satisfy the following conditions:

- a) the material is weightless and subjected to no body forces;
- b) the material is homogeneous, isotropic and linearly elastic;
- c) that the conditions are those of plane strain; and
- d) the medium is infinite or closed by a finite external boundary of arbitrary shape.

The medium may contain a number of excavations of arbitrary shape. The loading may consist of any combination of uniformly distributed loads on the boundaries, and in the case of an infinite medium, loads may also be present in the form of uniform field stresses.

There is provision to take advantage of any symmetry of the problem in order to reduce data input and solution cost. The program can be used to determine energy released at different stages of excavation for an excavation composed of a number of holes of arbitrary shape.

The output consists of an echo of the input data, boundary and grid

point stresses and optional boundary and grid point displacements as well as the energy released due to different stages of excavations.

The sign convention adopted is the same as that used by Bray (1976). The compressive stresses are taken as positive and the sign convention for the displacements is as for the coordinates axes. The x coordinate axis is positive to the right hand-side and the z axis is positive to the downward position.

#### INPUT DATA

A line by line description of the input data is presented in this section. The input data is in free format which ensures the friendliness of the program. The data can be input through screen or through data file (batch job). When the input data is input through screen, the input data will be stored in a data file. The data file provides a record of the input data.

#### INPUT DATA DESCRIPTION

Line 1 NPROB - Number of problems to be analyzed.

Line 2 TITLE - TITLE of each analysis (max. 80 characters).

Line 3 KEYA - is for debug control and should be set to 0.

Line 4 KEYB - controls the generation of a plot file. NOT supported. KEYB=0

Line 5 KEYC - controls the calculation of displacements.

If 0, no displacements are calculated.

If 1, displacements are calculated at the same points as are stresses.

The calculation of displacements approximately doubles the cost of the run. Note that displacements are always calculated at specified extra points. The presence of any extra points will force the calculation of displacements at the boundary regardless of KEYC.

When KEYC = 0, no energy will be calculated except when KEYD > 0.

Line 6 KEYD - controls the calculation of stresses and displacements at specified extra points.

If 0, no extra points are included in the data.

If 1, extra points are included, and displacements are also output for points on the excavation boundary even if KEYC is set to 0.

Line 7 KEY - controls the program application of MBAR and CRIT.

If 0, the criterion for the selection of radial grid lines is the distance specified in CRIT, and KBAR is defaulted to 1

If 1, the radial grid lines are drawn at every Nth element where N is the value of KBAR and CRIT is not used.

If 2, KBAR and CRIT are used as specified and in that order.

Line 8 KBAR - controls the radial spacing of the grid lines, which are drawn from the centre of element number 1,  $1 + \text{KBAR}$ ,  $1 + 2 * \text{KBAR}$ , etc.

Line 9 CRIT - is a floating point number. It is the minimum distance between radial grid lines at which stresses and displacements will be calculated.

Line 10 - NEXC, E, RNU, FPX, FPZ

NEXC is the number of stages of excavations.

E is the Young's modulus of the material.

RNU is the Poisson's ratio of the material.

FPX is the initial field stress on the region in the X-direction (compression positive).

FPZ is the initial field stress on the region in the Z-direction (compression positive).

Line 11 - NSEG, KXS, KZS, NCYC, NSL, DELN

where NSEG - is the number of elements.

KXS - controls symmetry about the X-axis.

If 0, the problem is not symmetrical about the X-axis.

If 1, the problem is symmetrical about the X-axis.

KZS - controls symmetry about the Z-axis.

If 0, the problem is not symmetrical about the Z-axis.

If 1, the problem is symmetrical about the Z-axis.

KCYC - is the number of cycles if iteration required.

KSL - is the number of grid lines parallel to the boundary on which stresses and displacements (optional) are to be calculated.

DELN - is the distance of the first parallel grid line from the boundary.

Line 12 - NUMEXC - is the number of elements that the newly exposed surface is composed of due to the excavation process.

Line 13 - NREF (NUMEXC) - are the element numbers of those elements at the newly exposed surface due to the excavation process.

Line 14 - NELR, XO, ZO, XL, ZL, RAD, RATIO PSI

This line describes the segment and element details. There are three types of segments - straight lines, circular arcs and elliptical arcs.

The first value on each line contains the number of elements into which the segments are to be divided. This is an integer and the remaining variables are real.

\* For each straight line segment the following data is required:

NELR is the number of elements.

XO is the X coordinate of the initial point of the segment.

ZO is the Z-coordinate of the initial point of the segment.

XL is the X-coordinate of the final point of the segment.

ZL is the Z-coordinate of the final point of the segment.

\* For each circular segment the following data is required.

NELR is the number of elements.

XO is the X-coordinate of the centre of the circle.

ZO is the Z-coordinate of the centre of the circle.

XL is the polar angle of the initial point measured in degrees anti-clockwise from the Z-axis.

ZL is the polar angle of the final point measured in degrees anti-clockwise from the Z-axis.

RAD is the radius of the circular arc.

\* For each elliptical segment the following data is required.

NELR is the number of elements.

XO is the X-coordinate of the centre of the ellipse.

Z0 is the Z-coordinate of the centre of the ellipse.

XL is the polar angle of the initial point measured in degrees anti-clockwise from the Z-axis.

ZL is the polar angle of the final point measured in degrees anti-clockwise from the Z-axis.

RAD is the length of one semi-axis (a).

RATIO is the ratio  $b/a$  where b is the length of the other semi-axis.

PSI is the polar angle of the semi-axis (a) measured in degrees anti-clockwise from the Z-axis.

There is one line for each segment and the total number of segments must correspond with the value entered on Line 11 on NSEG.

The segments of all openings must be coded in an anti-clockwise direction, although the starting point is immaterial. It should be noted that for a circular or elliptical segment, the polar angle of the final point must be greater than that of the initial point and cannot exceed  $360^{\circ}$ . Thus, a closed form can only be specified for  $0-360^{\circ}$ , and in the case of segments where the polar angle of the final point is less than that of the initial, a subdivision into two segments must be made. For example, a segment of range  $270^{\circ}-40^{\circ}$  must be split into segments  $270^{\circ}-360^{\circ}$  and  $0^{\circ}-40^{\circ}$ .

Each opening should be coded as a unit and it is advantageous to list the segments consecutively in an anti-clockwise order, irrespective of segment type.

Line 15 - LP1, LP2, BPX, BPZ, LPC (NOT SUPPORTED FOR ENERGY CALCULATIONS)

Additional loads may be specified as acting at the centre of any boundary element.

LP1 - is the first element number (not segment) over which the load is applied.

LP2 - is the last element number over which the load is applied.

BPX - is the X component or component parallel to the direction of the element of the total force on the element.

BPZ - is the Z component or component perpendicular to the direction of the element of the total force on the element.

LPC - determines the resolution of the force. If 0, component of force are parallel to X and Z axes. If 1, component of force are perpendicular and parallel to the element.

The boundary load data are terminated by a line with five zeros. This line with 5 zeros must always be present even if there are no boundary loads.

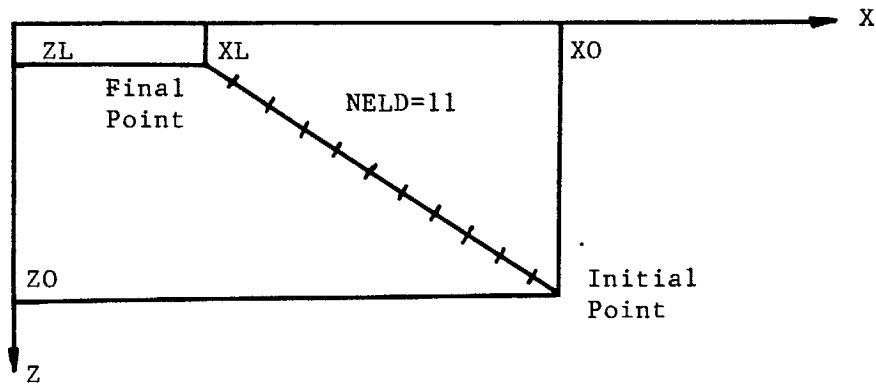


Fig. A-3 - Example of straight line segment.

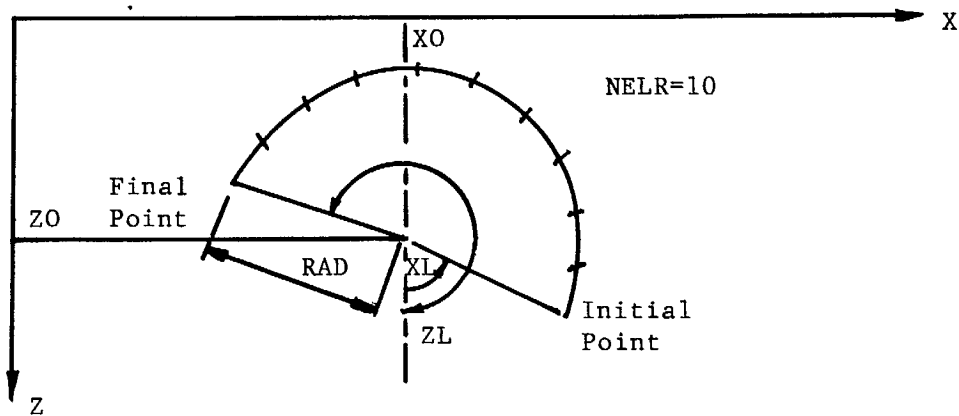


Fig. A-4 - Example of circular segment.

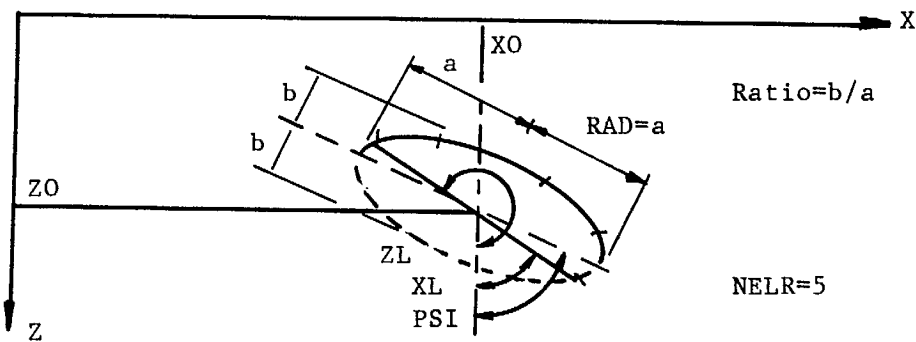


Fig. A-5 - Example of elliptical segment.

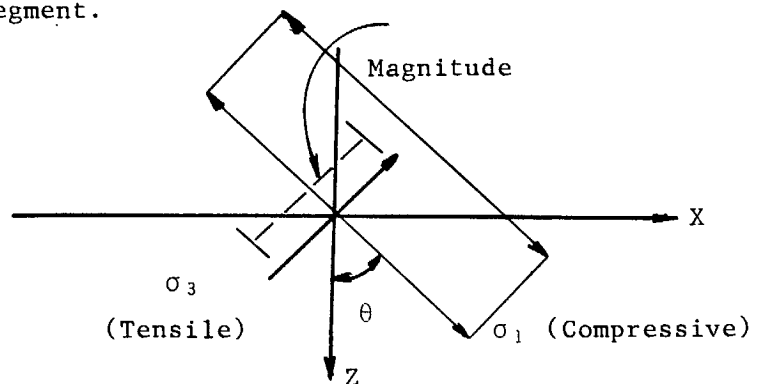


Fig. A-6 - Principal stresses.



Line 16 - NBS, CX1, CZ1, CX2, CZ2

This line describes the location of additional points where stresses and displacements are calculated.

NBS - Number of elements in the line segment.

CX1 - is the X coordinate of the starting point of the line segment.

CZ1 - is the Z coordinate of the starting point of the line segment.

CX2 - is the X coordinate of the ending point of the line segment.

CZ2 - is the Z coordinate of the ending point of the line segment.

This input terminated with  $NBS \geq 9999$ . e.g., 999, 0.0, 0.0, 0.0, 0.0.

OUTPUT: The sign conventions for the output of element and grid-point displacements and stresses are identical with those for the program BEM 2D version 2.2.

#### Stress Displacements at the Centre of Each Boundary Element

The element number is given, together with the X and Z coordinates of the centre of the element and the major and minor principal stresses, together with the angle which the major principal stress makes with the normal to the element.

Where there are no boundary loads on the excavation the minor principal stress should be zero and the angle should be  $\pm 90^\circ$ . This gives a good indication whether sufficient cycles were allowed for the iterative solution. The displacements have the same orientation and sign convention as the axes.

#### Stress and Optional Displacements at Grid Points Generated Automatically by the Program

The results appear in sets, one for each grid line generated parallel to the boundary.

The stresses appear as major and minor principal stresses, together with the angle that the major principal stress makes with the Z-axis (see Figure A-4). This differs from the angle definition given above for the

boundary stresses. The coordinates of the point are given together with an identifying integer number.

If required, displacements at the same point are given, together with a repeat of the coordinates of the point.

#### REFERENCES

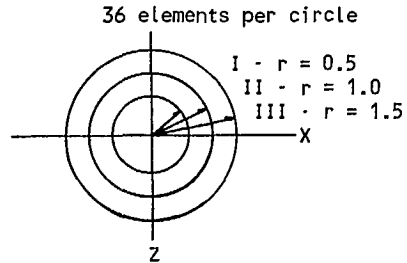
Bray, J.W., (1976), A program for two-dimensional stress analysis using the boundary element method, Progress Report No. 16, Rock Mechanics Project, Imperial College.

Salamon, M.D.G. (1984), Energy considerations in rock mechanics; fundamental results; J. S. Afr. Inst. Min. Met., vol. 84, No. 8, pp. 233-246.

INPUT - OUTPUT EXAMPLE

```
*****
*
* A computer program for determining the energy released from
* excavations utilizing the fictitious force indirect boundary
* element method of Bray based on Salamons energy formulation
* 2D Analysis -- Plane Strain Conditions
*
* For the units of metres and Megapascals, the units of the
* calculated energy are Mega Joules per metre of excavation.
*****
```

TITLE: CIRCULAR OPENING -- 3 EXCAVATION STAGES  
 -----



\*\*\* PROBLEM NO. 1

CONTROL OPTIONS SET TO:  
 -----

DISPLACEMENTS= 1 ,EXTRA COORDS.= 0

SELECTION SWITCHES FOR INTERIOR GRID POINTS:  
 KEY,KBAR,CRITERIA= 0 0 .000

NO. OF EXCA, E, RNU, FPX, FPZ = 3 70000.0 .25 100.0 100.0

EXCAVATION STAGE NO. = 1 --- INPUT SUMMARY

NSEG, KXS, KZS, NCYC, NSL, DELN= 1 0 0 40 0 .000

NO. OF ELEMENTS - NEW EXCA. = 36

ELEMENT NOS. OF NEW EXCA =	1	2	3	4	5	6	7	8
	9	10	11	12	13	14	15	16
	17	18	19	20	21	22	23	24
	25	26	27	28	29	30	31	32
	33	34	35	36				

ELEMENTS	CENT X	CENT Z	THET1	THET2	RADIUS	RATIO	PSI
36	.000	.000	.000	360.000	.500	1.000	.000

EXCAVATION STAGE NO. = 2 --- INPUT SUMMARY

NSEG, KXS, KZS, NCYC, NSL, DELN= 1 0 0 40 0 .000

NO. OF ELEMENTS - NEW EXCA. = 36

ELEMENT NOS. OF NEW EXCA =

1	2	3	4	5	6	7	8
9	10	11	12	13	14	15	16
17	18	19	20	21	22	23	24
25	26	27	28	29	30	31	32
33	34	35	36				

ELEMENTS	CENT X	CENT Z	THET1	THET2	RADIUS	RATIO	PSI
36	.000	.000	.000	360.000	1.000	1.000	.000

EXCAVATION STAGE NO. = 3 --- INPUT SUMMARY

NSEG, KXS, KZS, NCYC, NSL, DELN= 1 0 0 40 0 .000

NO. OF ELEMENTS - NEW EXCA. = 36

ELEMENT NOS. OF NEW EXCA =

1	2	3	4	5	6	7	8
9	10	11	12	13	14	15	16
17	18	19	20	21	22	23	24
25	26	27	28	29	30	31	32
33	34	35	36				

ELEMENTS	CENT X	CENT Z	THET1	THET2	RADIUS	RATIO	PSI
36	.000	.000	.000	360.000	1.500	1.000	.000

\*\*\*\*\* STAGE NO. 1 \*\*\*\*\*

STRESSES AT CENTRES OF BOUNDARY ELEMENTS

1	CX	CZ	SIG1	SIG3	ALPHA	ES30	SIGM
1	.04	.50	200.0	.0	90.0	200.0	100.0
2	.13	.48	200.0	.0	90.0	200.0	100.0
3	.21	.45	200.0	.0	90.0	200.0	100.0
4	.29	.41	200.0	.0	90.0	200.0	100.0
5	.35	.35	200.0	.0	90.0	200.0	100.0
6	.41	.29	200.0	.0	90.0	200.0	100.0
7	.45	.21	200.0	.0	90.0	200.0	100.0
8	.48	.13	200.0	.0	90.0	200.0	100.0
9	.50	.04	200.0	.0	90.0	200.0	100.0
10	.50	-.04	200.0	.0	90.0	200.0	100.0

11	.48	-.13	200.0	.0	90.0	200.0	100.0
12	.45	-.21	200.0	.0	90.0	200.0	100.0
13	.41	-.29	200.0	.0	90.0	200.0	100.0
14	.35	-.35	200.0	.0	90.0	200.0	100.0
15	.29	-.41	200.0	.0	90.0	200.0	100.0
16	.21	-.45	200.0	.0	90.0	200.0	100.0
17	.13	-.48	200.0	.0	90.0	200.0	100.0
18	.04	-.50	200.0	.0	90.0	200.0	100.0
19	-.04	-.50	200.0	.0	90.0	200.0	100.0
20	-.13	-.48	200.0	.0	90.0	200.0	100.0
21	-.21	-.45	200.0	.0	90.0	200.0	100.0
22	-.29	-.41	200.0	.0	90.0	200.0	100.0
23	-.35	-.35	200.0	.0	90.0	200.0	100.0
24	-.41	-.29	200.0	.0	90.0	200.0	100.0
25	-.45	-.21	200.0	.0	90.0	200.0	100.0
26	-.48	-.13	200.0	.0	90.0	200.0	100.0
27	-.50	-.04	200.0	.0	90.0	200.0	100.0
28	-.50	.04	200.0	.0	90.0	200.0	100.0
29	-.48	.13	200.0	.0	90.0	200.0	100.0
30	-.45	.21	200.0	.0	90.0	200.0	100.0
31	-.41	.29	200.0	.0	90.0	200.0	100.0
32	-.35	.35	200.0	.0	90.0	200.0	100.0
33	-.29	.41	200.0	.0	90.0	200.0	100.0
34	-.21	.45	200.0	.0	90.0	200.0	100.0
35	-.13	.48	200.0	.0	90.0	200.0	100.0
36	-.04	.50	200.0	.0	90.0	200.0	100.0

## DISPLACEMENTS AT CENTRES OF BOUNDARY ELEMENTS

I	CX	CZ	UX (cm)	UZ (cm)
1	.04	.50	-.0081	-.0922
2	.13	.48	-.0239	-.0894
3	.21	.45	-.0391	-.0838
4	.29	.41	-.0531	-.0758
5	.35	.35	-.0654	-.0654
6	.41	.29	-.0758	-.0531
7	.45	.21	-.0838	-.0391
8	.48	.13	-.0894	-.0239
9	.50	.04	-.0922	-.0081
10	.50	-.04	-.0922	.0081
11	.48	-.13	-.0894	.0239
12	.45	-.21	-.0838	.0391
13	.41	-.29	-.0758	.0531
14	.35	-.35	-.0654	.0654
15	.29	-.41	-.0531	.0758
16	.21	-.45	-.0391	.0838
17	.13	-.48	-.0239	.0894
18	.04	-.50	-.0081	.0922
19	-.04	-.50	.0081	.0922
20	-.13	-.48	.0239	.0894
21	-.21	-.45	.0391	.0838
22	-.29	-.41	.0531	.0758
23	-.35	-.35	.0654	.0654
24	-.41	-.29	.0758	.0531
25	-.45	-.21	.0838	.0391
26	-.48	-.13	.0894	.0239
27	-.50	-.04	.0922	.0081
28	-.50	.04	.0922	-.0081
29	-.48	.13	.0894	-.0239
30	-.45	.21	.0838	-.0391
31	-.41	.29	.0758	-.0531
32	-.35	.35	.0654	-.0654
33	-.29	.41	.0531	-.0758
34	-.21	.45	.0391	-.0838
35	-.13	.48	.0239	-.0894
36	-.04	.50	.0081	-.0922

\*\*\*\*\* EXCA STAGE NO. = 1 ENERGY SUMMARY \*\*\*\*\*

Wk, Um, W, Uc, Wr = .145 .070 .430 .285 .215  
 SEISMIC EFFICIENCY= 67.5 %

\*\*\*\*\* STAGE NO. 2 \*\*\*\*\*

## STRESSES AT CENTRES OF BOUNDARY ELEMENTS

I	CX	CZ	SIG1	SIG3	ALPHA	ES30	SIGM
1	.09	.99	200.0	.0	90.0	200.0	100.0
2	.26	.96	200.0	.0	90.0	200.0	100.0
3	.42	.90	200.0	.0	90.0	200.0	100.0
4	.57	.82	200.0	.0	90.0	200.0	100.0
5	.70	.70	200.0	.0	90.0	200.0	100.0
6	.82	.57	200.0	.0	90.0	200.0	100.0
7	.90	.42	200.0	.0	90.0	200.0	100.0
8	.96	.26	200.0	.0	90.0	200.0	100.0
9	.99	.09	200.0	.0	90.0	200.0	100.0
10	.99	-.09	200.0	.0	90.0	200.0	100.0
11	.96	-.26	200.0	.0	90.0	200.0	100.0
12	.90	-.42	200.0	.0	90.0	200.0	100.0
13	.82	-.57	200.0	.0	90.0	200.0	100.0
14	.70	-.70	200.0	.0	90.0	200.0	100.0
15	.57	-.82	200.0	.0	90.0	200.0	100.0
16	.42	-.90	200.0	.0	90.0	200.0	100.0
17	.26	-.96	200.0	.0	90.0	200.0	100.0
18	.09	-.99	200.0	.0	90.0	200.0	100.0
19	-.09	-.99	200.0	.0	90.0	200.0	100.0
20	-.26	-.96	200.0	.0	90.0	200.0	100.0
21	-.42	-.90	200.0	.0	90.0	200.0	100.0
22	-.57	-.82	200.0	.0	90.0	200.0	100.0
23	-.70	-.70	200.0	.0	90.0	200.0	100.0
24	-.82	-.57	200.0	.0	90.0	200.0	100.0
25	-.90	-.42	200.0	.0	90.0	200.0	100.0
26	-.96	-.26	200.0	.0	90.0	200.0	100.0
27	-.99	-.09	200.0	.0	90.0	200.0	100.0
28	-.99	.09	200.0	.0	90.0	200.0	100.0
29	-.96	.26	200.0	.0	90.0	200.0	100.0
30	-.90	.42	200.0	.0	90.0	200.0	100.0
31	-.82	.57	200.0	.0	90.0	200.0	100.0
32	-.70	.70	200.0	.0	90.0	200.0	100.0
33	-.57	.82	200.0	.0	90.0	200.0	100.0
34	-.42	.90	200.0	.0	90.0	200.0	100.0
35	-.26	.96	200.0	.0	90.0	200.0	100.0
36	-.09	.99	200.0	.0	90.0	200.0	100.0

## DISPLACEMENTS AT CENTRES OF BOUNDARY ELEMENTS

I	CX	CZ	UX (cm)	UZ (cm)
1	.09	.99	-.0161	-.1843
2	.26	.96	-.0479	-.1787
3	.42	.90	-.0782	-.1677
4	.57	.82	-.1061	-.1516
5	.70	.70	-.1308	-.1308
6	.82	.57	-.1516	-.1061
7	.90	.42	-.1677	-.0782
8	.96	.26	-.1787	-.0479

9	.99	.09	-.1843	-.0161
10	.99	-.09	-.1843	.0161
11	.96	-.26	-.1787	.0479
12	.90	-.42	-.1677	.0782
13	.82	-.57	-.1516	.1061
14	.70	-.70	-.1308	.1308
15	.57	-.82	-.1061	.1516
16	.42	-.90	-.0782	.1677
17	.26	-.96	-.0479	.1787
18	.09	-.99	-.0161	.1843
19	-.09	-.99	.0161	.1843
20	-.26	-.96	.0479	.1787
21	-.42	-.90	.0782	.1677
22	-.57	-.82	.1061	.1516
23	-.70	-.70	.1308	.1308
24	-.82	-.57	.1516	.1061
25	-.90	-.42	.1677	.0782
26	-.96	-.26	.1787	.0479
27	-.99	-.09	.1843	.0161
28	-.99	.09	.1843	-.0161
29	-.96	.26	.1787	-.0479
30	-.90	.42	.1677	-.0782
31	-.82	.57	.1516	-.1061
32	-.70	.70	.1308	-.1308
33	-.57	.82	.1061	-.1516
34	-.42	.90	.0782	-.1677
35	-.26	.96	.0479	-.1787
36	-.09	.99	.0161	-.1843

\*\*\*\*\* EXCA STAGE NO. = 2 ENERGY SUMMARY \*\*\*\*\*

Wk, Um, W, Uc, Wr = .322 .314 1.272 .950 .636  
SEISMIC EFFICIENCY= 50.6 %

\*\*\*\*\* STAGE NO. 3 \*\*\*\*\*

STRESSES AT CENTRES OF BOUNDARY ELEMENTS

I	CX	CZ	SIG1	SIG3	ALPHA	ES30	SIGM
1	.13	1.49	200.0	.0	90.0	200.0	100.0
2	.39	1.44	200.0	.0	90.0	200.0	100.0
3	.63	1.35	200.0	.0	90.0	200.0	100.0
4	.86	1.22	200.0	.0	90.0	200.0	100.0
5	1.06	1.06	200.0	.0	90.0	200.0	100.0
6	1.22	.86	200.0	.0	90.0	200.0	100.0
7	1.35	.63	200.0	.0	90.0	200.0	100.0
8	1.44	.39	200.0	.0	90.0	200.0	100.0
9	1.49	.13	200.0	.0	90.0	200.0	100.0
10	1.49	-.13	200.0	.0	90.0	200.0	100.0
11	1.44	-.39	200.0	.0	90.0	200.0	100.0
12	1.35	-.63	200.0	.0	90.0	200.0	100.0
13	1.22	-.86	200.0	.0	90.0	200.0	100.0
14	1.06	-1.06	200.0	.0	90.0	200.0	100.0
15	.86	-1.22	200.0	.0	90.0	200.0	100.0
16	.63	-1.35	200.0	.0	90.0	200.0	100.0
17	.39	-1.44	200.0	.0	90.0	200.0	100.0
18	.13	-1.49	200.0	.0	90.0	200.0	100.0
19	-.13	-1.49	200.0	.0	90.0	200.0	100.0
20	-.39	-1.44	200.0	.0	90.0	200.0	100.0
21	-.63	-1.35	200.0	.0	90.0	200.0	100.0
22	-.86	-1.22	200.0	.0	90.0	200.0	100.0

23	-1.06	-1.06	200.0	.0	90.0	200.0	100.0
24	-1.22	-.86	200.0	.0	90.0	200.0	100.0
25	-1.35	-.63	200.0	.0	90.0	200.0	100.0
26	-1.44	-.39	200.0	.0	90.0	200.0	100.0
27	-1.49	-.13	200.0	.0	90.0	200.0	100.0
28	-1.49	.13	200.0	.0	90.0	200.0	100.0
29	-1.44	.39	200.0	.0	90.0	200.0	100.0
30	-1.35	.63	200.0	.0	90.0	200.0	100.0
31	-1.22	.86	200.0	.0	90.0	200.0	100.0
32	-1.06	1.06	200.0	.0	90.0	200.0	100.0
33	-.86	1.22	200.0	.0	90.0	200.0	100.0
34	-.63	1.35	200.0	.0	90.0	200.0	100.0
35	-.39	1.44	200.0	.0	90.0	200.0	100.0
36	-.13	1.49	200.0	.0	90.0	200.0	100.0

## DISPLACEMENTS AT CENTRES OF BOUNDARY ELEMENTS

I	CX	CZ	UX (cm)	UZ (cm)
1	.13	1.49	-.0242	-.2765
2	.39	1.44	-.0718	-.2681
3	.63	1.35	-.1173	-.2515
4	.86	1.22	-.1592	-.2273
5	1.06	1.06	-.1963	-.1963
6	1.22	.86	-.2273	-.1592
7	1.35	.63	-.2515	-.1173
8	1.44	.39	-.2681	-.0718
9	1.49	.13	-.2765	-.0242
10	1.49	-.13	-.2765	.0242
11	1.44	-.39	-.2681	.0718
12	1.35	-.63	-.2515	.1173
13	1.22	-.86	-.2273	.1592
14	1.06	-1.06	-.1963	.1963
15	.86	-1.22	-.1592	.2273
16	.63	-1.35	-.1173	.2515
17	.39	-1.44	-.0718	.2681
18	.13	-1.49	-.0242	.2765
19	-.13	-1.49	.0242	.2765
20	-.39	-1.44	.0718	.2681
21	-.63	-1.35	.1173	.2515
22	-.86	-1.22	.1592	.2273
23	-1.06	-1.06	.1963	.1963
24	-1.22	-.86	.2273	.1592
25	-1.35	-.63	.2515	.1173
26	-1.44	-.39	.2681	.0718
27	-1.49	-.13	.2765	.0242
28	-1.49	.13	.2765	-.0242
29	-1.44	.39	.2681	-.0718
30	-1.35	.63	.2515	-.1173
31	-1.22	.86	.2273	-.1592
32	-1.06	1.06	.1963	-.1963
33	-.86	1.22	.1592	-.2273
34	-.63	1.35	.1173	-.2515
35	-.39	1.44	.0718	-.2681
36	-.13	1.49	.0242	-.2765

\*\*\*\*\* EXCA STAGE NO. = 3 ENERGY SUMMARY \*\*\*\*\*

Wk, Um, W, Uc, Wr = .389 .650 2.078 1.688 1.039  
 SEISMIC EFFICIENCY= 37.5 %



A closed - form solution exists for this example (Salamon, 1974). The seismic energy ( $W_k$ ) and the stored strain energy ( $U_m$ ) can be expressed by.

$$W_k = (1+u)(1-a^2/c^2)\pi(c^2-a^2)p^2/E \quad A4.$$

$$U_m = (1+u)(1-2u+a^2/c^2)\pi(c^2-a^2)p^2/E \quad A5.$$

where

- a = initial tunnel radius
- c = enlarged tunnel radius
- p = hydrostatic stress
- E = elastic modulus
- u = Poisson's ratio

The results from the computer model and equations A4. and A5. are compared in Table A1.

Table A1. : Comparison of Energy Components for a Circular Opening under Hydrostatic Stress

Model	a = 0, c = 0.5m		a = 0.5m, c = 1.0m		a = 1.0m, c = 1.5m	
	$W_k$	$U_m$	$W_k$	$U_m$	$W_k$	$U_m$
EXENBRAY	0.145	0.070	0.322	0.314	0.389	0.650
Closed-form	0.140	0.070	0.316	0.316	0.390	0.662

The maximum discrepancy is 3.6 %, and if more elements are used in the computer model the discrepancy decreases.

The execution time to run the above example is about 75 minutes on an IBM PC system without an 8087 NDP Coprocessor and only 5 minutes with the Coprocessor.



```

5041 continue
C
C  ** SET ARRAY SIZE LIMIT **
C
      LMTARA=300
c      READ(*,540) NPR0B
      if(nopt.eq.2)write(*,5001)
5001 format(1x,'NUMBER OF PROBLEM ?')
      read(in,*) nprob
      540 FORMAT(15)
      if(nopt.eq.2)write(is,*)nprob
      WRITE(io,320)
      write(io,3191)
      320 format(1h ,//5x,68(1h*),/5x,1h*,66x,1h*,/5x,4h*
1 'A computer program for determining the energy released from',
1 5h *,/5x,4h* , 'excavations utilizing the fictitious'
1 ,1x,'force indirect boundary',3h *,/5x,4h* ,
1 'element method of Bray based on Salamons energy formulation',
1 5H *,/5x,4h* , '2D Analysis -- Plane Strain Conditions',
1 25x,1h*,/5x,1h*,66x,1h*)
3191 format(5x,4h* , 'For the units of metres and',
1 1x,'Megapascals, the units of the',7h *,/5x,4h* ,
1 'calculated energy are Mega Joules per metre of excavation.',
1 6h *,/5x,1h*,66x,1h*,/5x,68(1h*))
c 320 FORMAT(1H1,/5X,81(1H*),/5X,1H*,79X,1H*,/5X,4H* ,
c 173H2D STRESS ANALYSIS BY BOUNDARY ELEMENT METHOD - PLANE STRAIN
c 2CONDITIONS, 4H *,/5X,1H*,79X,1H*,/5X,81(1H*))
      N = 0
C
C  ** SET STARTING POINT FOR NEXT PROBLEM **
C
31415 CONTINUE
      N = N + 1
      IF(N.GT.NPROB) STOP
C
C  ** SET SWITCH FOR PROCESSING BOUNDARY POINTS **
C
      KSWH=0
      if(nopt.eq.2)write(*,5002)
5002 format(1x,'JOB TITLE ? (max 80 characters)')
      read(in,10) TITLE
      if(nopt.eq.2)write(is,10)title
      10 format(20a4)
      write(io,9)TITLE
C
C-----
C
C  ***** INPUT DATA FROM FILE 'TWOBE.DAT' *****
C-----
C
      if(nopt.eq.1)go to 3001
      write(*,3002)
3002 format(1x,'INPUT KEYA ?',//,1x,'KEYA IS FOR DEBUG CONTROL AND'
1 , ' SHOULD BE SET TO ZERO.')
      read(in,*)keya
      write(is,*)keya
      write(*,3003)
3003 format(1x,'INPUT KEYB ?',//,1x,'KEYB CONTROLS THE GENERATION',
1 ' OF A PLOT FILE --- NOT SUPPORTED INPUT ZERO')
      read(in,*)keyb
      write(is,*)keyb
      write(*,3004)
3004 format(1x,'INPUT KEYC ?',//,1x,'KEYC CONTROLS THE CALCULATION',
1 ' OF DISPLACEMENTS.',//,1x,
1 ' IF 0, NO DISPLACEMENTS ARE CALCULATED AND NO ENERGY ',
1 ' RELEASED WILL BE CALCULATED EXCEPT KEYD > 0.',//,1x,
1 ' IF 1, DISPLACEMENTS ARE CALCULATED AT THE SAME POINTS AS',
1 ' STRESSES.')
      read(in,*)keyc
      write(is,*)keyc
      write(*,3005)

```

```

3005 format(1x,'INPUT KEYD ?',//,1x,'KEYD CONTROLS THE CALCULATIONS',
1 ' OF STRESSES AND DISPLACEMENTS AT SPECIFIED EXTRA POINTS',//,
1 ' IF 0, NO EXTRA POINTS ARE INCLUDED IN THE ANALYSIS.'//,1x,
1 ' IF 1, EXTRA POINTS ARE INCLUDED, AND DISPLACEMENTS ARE ALSO'//
1 1x,'OUTPUT FOR POINTS ON THE EXCAVATION BOUNDARY EVEN IF KEYC=0')
read(in,*)keyd
write(is,*)keyd
write(*,3006)
3006 format(1x,'INPUT KEY ?',//,1x,'KEY CONTROLS THE PROGRAM APPLICATION',
1 ' OF KBAR AND CRIT,'//,1x,'IF 0, THE CRITERION FOR THE SELECTION',
1 ' OF THE RADIAL GRID LINES IS THE DISTANCE'//,1x,'SPECIFIED IN'
1 ' CRIT, AND KBAR IS DEFAULTED TO 1.'//,1x,'IF 1, THE RADIAL GRID',
1 ' LINES ARE DRAWN AT EVERY Nth ELEMENT WHERE N IS THE VALUE'//,1x,
1 ' OF KBAR AND CRIT IS NOT USED.'//,1x,'IF 2, KBAR AND CRIT ARE'
1 ' USED AS SPECIFIED AND IN THAT ORDER.')
read(in,*)key
write(is,*)key
write(*,3007)
3007 format(1x,'INPUT KBAR ?',//,1x,'KBAR CONTROLS THE RADIAL SPACING',
1 ' OF THE GRID LINES,'//,1x,'WHICH ARE DRAWN FROM THE CENTRE OF ',
1 ' ELEMENT NUMBER 1, 1+KBAR,*'//,1x,'1+2*KBAR ETC.')
```

```

read(in,*)kbar
write(is,*)kbar
write(*,3008)
3008 format(1x,'INPUT CRIT ?',//,1x,'CRIT IS THE MINIMUM DISTANCE',
1 ' BETWEEN RADIAL GRID LINES AT'//,1x,'WHICH STRESSES AND',
1 ' DISPLACEMENTS WILL BE CALCULATED. IT IS DESCRIBED IN'//,
1 1x,'DETAIL IN USER MANUAL.')
read(in,*)crit
write(is,*)crit
c READ(in,*) KEYA,KEYB,KEYC,KEYD,KEY,KBAR,CRIT
3001 continue
if(nopt.eq.2) go to 3040
read(in,*)keya
read(in,*)keyb
read(in,*)keyc
read(in,*)keyd
read(in,*)key
read(in,*)kbar
read(in,*)crit
3040 continue
545 FORMAT(6I5,F10.0)
WRITE(io,200) N,KEYC,KEYD,KEY,KBAR,CRIT
200 FORMAT(///// ' *** PROBLEM NO.',13,///' CONTROL OPTIONS SET TO:',
1/1X,23(1H-),///' DISPLACEMENTS=',12,' , EXTRA COORDS.',12,
2 ///' SELECTION SWITCHES FOR INTERIOR GRID POINTS:'
3 /20X,'KEY,KBAR,CRITERIA=',213,F10.3)
KBAR= MAX0(1,KBAR)
c READ(5,10) TITLE
c 10 FORMAT(20A4)
c WRITE(io,9) TITLE
9 FORMAT(1H ,////' TITLE: ',20A4,/1X,6(1H-))
c READ(5,11) NSEG,KXS,KZS,NCYC,NSL,DELN,E,RNU,FPX,FPZ
11 FORMAT(5I5,5G10.0)
if(nopt.eq.2)write(*,5003)
5003 format(1x,'NO OF EXCAVATIONS, E, RNU, FPX, FPZ?')
read(in,*)nexc,e,rnu,fpz
if(nopt.eq.2)write(is,*)nexc,e,rnu,fpz
write(io,1113)nexc,e,rnu,fpz
1113 format(1h //,' NO. OF EXCA, E, RNU, FPX, FPZ = ',
1 13,3x,f7.1,3x,f3.2,2f8.1)
C
C ** IF E= 0, THEN IT IS ARBITRARILY SET TO 20000.0
C
C IF(E.LE.0.) E=20000.
C
C WRITE(io,13)NSEG,KXS,KZS,NCYC,NSL,DELN,E,RNU,FPX,FPZ
c 13 FORMAT(1H ///,7X,28HNSEG, KXS, KZS, NCYC, NSL = ,516 ///,
c 1 7X,26HDELN, E , RNU, FPX, FPZ = ,F10.3,E12.4,3F10.3///)
NN = 0
PI = 3.1415926
TA = 2.0*(1.0 - RNU)

```

```

TJ = 1.0/(2.0*PI*TA)
TU=3.0-4.0*RNU
G=E/(2.0*(1.0+RNU))
TV=0.5*TJ/G
TW=(1.0-RNU*RNU)/E
TX=RNU/(1.0-RNU)
C
C  ** INTERPRETATION OF SYMMETRY CODE **
do 9991 nxt=1,nexc
write(io,5030)nxt
5030 format(1h ///,16x,'EXCAVATION STAGE NO. = ',i2,
1 ' --- INPUT SUMMARY')
if(nopt.eq.2)write(*,3010)nxt
3010 format(1x,'INPUT FOR EXCAVATION STAGE =',i3)
if(nopt.eq.2)write(*,5004)
5004 format(1h //,' NSEG, KXS, KZS, NCYC, NSL, DELN?')
read(in,*)nseg,kxs,kzs,ncyc,nsl(nxt),deln(nxt)
if(nopt.eq.2)write(is,*)nseg,kxs,kzs,ncyc,nsl(nxt),deln(nxt)
write(io,1114)nseg,kxs,kzs,ncyc,nsl(nxt),deln(nxt)
1114 format(1h //,' NSEG, KXS, KZS, NCYC, NSL, DELN=',
1 5i5,f10.3)
if(nexc.eq.1) go to 9993
if(nopt.eq.2)write(*,5005)
5005 format(' NO. OF ELEMENTS THE NEWLY EXPOSED SURFACE CONSISTS OF?')
read(in,*)numexc(nxt)
if(nopt.eq.2)write(is,*)numexc(nxt)
write(io,1115)numexc(nxt)
1115 format(1h //,' NO. OF ELEMENTS - NEW EXCA. =',
1 i5)
if(nopt.eq.2)write(*,5006)
5006 format(' ELEMENT NOS. OF THE NEWLY EXPOSED SURFACE?')
read(in,*)(nref(kk,nxt),kk=1,numexc(nxt))
if(nopt.eq.2)write(is,*)(nref(kk,nxt),kk=1,numexc(nxt))
write(io,1116)(nref(kk,nxt),kk=1,numexc(nxt))
1116 format(1h //,' ELEMENT NOS. OF NEW EXCA = ',
1 1x,8i5,8(/29x,8i5))
write(io,1999)
1999 format(///)
9993 continue
C
KAS(nxt) = 0
IF(KZS.EQ.-1) KAS(nxt) = 1
KXT(nxt) = 2*KXS + 1
KZT(nxt) = 2*(KZS + KAS(nxt)) + 1
C
-----
C
C ***** DIVISION OF BOUNDARY SEGMENTS INTO ELEMENTS *****
C
-----
C
I = 0
NSEGG = 0
700 IF(NSEGG.EQ.NSEG) GO TO 50
NSEGG = NSEGG + 1
NELG = 0
if(nopt.eq.2)write(*,5008)
5008 format(' NELR, XO, ZO, XL, ZL, RAD, RATIO, PSI?')
READ(in,*) NELR,XO,ZO,XL,ZL,RAD,RATIO,PSI
if(nopt.eq.2)write(is,*)nelr,xo,zo,xl,zl,rad,ratio,psi
17 FORMAT(7X,13,7F10.0)
IF(RAD.LT.1E-8) GOTO 800
C
C ** DIVISION OF ELLIPTICAL OR CIRCULAR SEGMENTS INTO ELEMENTS **
C
IF(RATIO.LT.1E-8) RATIO=1.0
WRITE(io,16)
16 FORMAT(1H ///,5X,8HELEMENTS,1X,6HCENT X,4X,6HCENT Z,5X,5HTHET1,
+ 5X,5HTHET2,5X,6HRADIUS,4X,5HRATIO,5X,3HPSI )
WRITE(io,18) NELR,XO,ZO,XL,ZL,RAD,RATIO,PSI
18 FORMAT(1H ,6X,13,7F10.3,/)
SINPSI = SIN(PSI*PI/180.)

```

```

COSPSI = COS(PSI*PI/180.)
GD=RAD/10000.
GA=RATIO*COS((XL-PSI)*PI/180.)
IF(ABS(GA).LT.GD) GA=GD
GB=RATIO*COS((ZL-PSI)*PI/180.)
IF(ABS(GB).LT.GD) GB=GD
CHI1=ATAN2(SIN((XL-PSI)*PI/180.),GA)
CHI2=ATAN2(SIN((ZL-PSI)*PI/180.),GB)
DCHI = (CHI2 - CHI1)/NELR
IF(ABS(DCHI).LT.GD) GOTO 606
GC=DCHI/ABS(DCHI)
GOTO 605
606 GC=-1.0
605 DCHI=DCHI+((ZL-XL)/ABS(ZL-XL)-GC)*PI/NELR
600 I = I + 1
CHI = CHI1 + NELG*DCHI
EX1(I,nxt) = RAD*(COS(CHI)*SINPSI + SIN(CHI)*COSPSI*RATIO) + XO
EZ1(I,nxt) = RAD*(COS(CHI)*COSPSI - SIN(CHI)*SINPSI*RATIO) + ZO
CHI = CHI + DCHI
EX2(I,nxt) = RAD*(COS(CHI)*SINPSI + SIN(CHI)*COSPSI*RATIO) + XO
EZ2(I,nxt) = RAD*(COS(CHI)*COSPSI - SIN(CHI)*SINPSI*RATIO) + ZO
C
CX(I,nxt) = 0.5*(EX1(I,nxt) + EX2(I,nxt))
CZ(I,nxt) = 0.5*(EZ1(I,nxt) + EZ2(I,nxt))
DX = EX2(I,nxt) - EX1(I,nxt)
DZ = EZ2(I,nxt) - EZ1(I,nxt)
SINB(I,nxt) = -DZ/SQRT(DX*DX + DZ*DZ)
COSB(I,nxt) = DX/SQRT(DX*DX + DZ*DZ)
NELG = NELG + 1
IF(NELG.LT.NELR) GO TO 600
GO TO 700
C
C ** DIVISION OF STRAIGHT SEGMENTS INTO ELEMENTS **
C
800 WRITE(io,14)
14 FORMAT(1H ,4X,8HELEMENTS,1X,6HFIRSTX,4X,6HFIRSTZ,5X,5HLASTX,5X,
+ 5HLASTZ )
WRITE(io,15) NELR,XO,ZO,XL,ZL
15 FORMAT(1H ,6X,I3,4F10.3,/)
C
DX = (XL-XO)/NELR
DZ = (ZL-ZO)/NELR
DS = SQRT(DX*DX + DZ*DZ)
900 I = I + 1
SINB(I,nxt) = -DZ/DS
COSB(I,nxt) = DX/DS
EX1(I,nxt) = XO + NELG*DX
EZ1(I,nxt) = ZO + NELG*DZ
CX(I,nxt) = EX1(I,nxt) + 0.5*DX
CZ(I,nxt) = EZ1(I,nxt) + 0.5*DZ
EX2(I,nxt) = EX1(I,nxt) + DX
EZ2(I,nxt) = EZ1(I,nxt) + DZ
NELG = NELG + 1
IF(NELG.LT.NELR) GO TO 900
GO TO 700
50 CONTINUE
C
c MAXI = I
c MAXJ = I
maxi9(nxt)=i
maxj9(nxt)=i
9991 continue
do 9992 nxt=1,nexc
if(nexc.gt.1)write(io,3303)nxt
3303 format(1h ///,27x,'***** STAGE NO. ',i3,' *****')
nn=c
ksw=0
ncal=0
nhcal=0
maxi=maxi9(nxt)
maxj=maxj9(nxt)
C

```

```

C-----
C
C ***** DETERMINATION OF BOUNDARY TRACTIONS *****
C-----
C
C ** TRACTIONS EQUIVALENT TO FIELD STRESSES **
C
DO 100 I = 1,MAXI
PM(I) = 2.0 * (FPX* COSB(I,nxt) **2 + FPZ* SINB(I,nxt) **2)
PN(I) = 2.0 * (FPZ* COSB(I,nxt) **2 + FPX* SINB(I,nxt) **2)
PNM(I) = 2.0*(FPX - FPZ)*SINB(I,nxt)*COSB(I,nxt)
QM(I) = PNM(I)
QN(I) = PN(I)
100 CONTINUE
C
C ** ADDITION OF BOUNDARY TRACTIONS DUE TO BOUNDARY LOADS **
C
106 continue
if(nopt.eq.2)write(*,5009)nxt
5009 format(1x,'STAGE No.=',i3,/,1x,'INPUT LP1, LP2, BPX, BPZ, LPC?')
READ(in,*) LP1,LP2,BPX,BPZ,LPC
if(nopt.eq.2)write(is,*)lp1,lp2,bpx,bpz,lpc
19 FORMAT(7X,I3,7X,I3,2F10.0,7X,I3)
IF(LP1.EQ.0) GO TO 105
WRITE(io,20) LP1,LP2,BPX,BPZ
20 FORMAT(1H ,6X,21HLP1, LP2, BPX, BPZ = ,2I6,2F10.3 ///)
DO 107 I = LP1,LP2
IF(LPC.GT.0) GO TO 120
PM(I) = PM(I) - 2.0*((BPX-BPZ)* COSB(I,nxt) **2 + BPZ
PN(I) = PN(I) - 2.0*((BPX-BPZ)* SINB(I,nxt) **2 + BPZ)
PNM(I) = PNM(I) - 2.*(BPX-BPZ)*SINB(I,nxt)*COSB(I,nxt)
GO TO 121
120 PN(I)=PN(I)-2.*BPZ
PNM(I)=PNM(I)-2.*BPX
121 CONTINUE
107 CONTINUE
GO TO 106
105 CONTINUE
655 CONTINUE
C-----
C
C ***** DETERMINATION OF FICTITIOUS LOADS *****
C-----
C
C ** COEFFICIENTS IN EXPRESSIONS FOR STRESSES INDUCED BY FICTITIOUS LOADS **
C
C
DO 101 I = 1,MAXI
do 101 jjk=1,maxi
i=jjk
nss=nxt
cxi=cx(i,nxt)
czi=cz(i,nxt)
if(ncal.ne.1) go to 9995
nss=nxt+1
i=nref(jjk,nss)
cxi=cx(i,nss)
czi=cz(i,nss)
9995 continue
c CXI = CX(I)
c CZI = CZ(I)
c IF(NN.GT.0) GO TO 104
if(nn.gt.0.and.ncal.eq.0) go to 104
COS2BI = 2.0 * COSB(I,nss) **2 - 1.0
SIN2BI = 2.0 * SINB(I,nss) * COSB(I,nss)
104 DO 101 J = 1,MAXJ
TK = 0.0
TL = 0.0
TM = 0.0
TN = 0.0

```

```

TO = 0.0
TP = 0.0
DO 102 KXU = 1,KXT(nxt),2
KX = 2 - KXU
DO 102 KZU = 1,KZT(nxt),2
KZ = (2-KZU)*(1-KAS(nxt)) + KAS(nxt)*KX
COSBJ = KX * COSB(J,nxt)
SINBJ = KZ * SINB(J,nxt)
RN = (CZI - KX*EZ1(J,nxt))*COSBJ + (CXI - KZ*EX1(J,nxt))*SINBJ
LL = KX + KZ - 2 + 10*(I-J) + 1000*NN
IF(LL.EQ.0) RN=SQRT((EX2(I,nss)-EX1(I,nss))**2
1 +(ez2(i,nss)-ez1(i,nss))**2)/10000.
RM1 = (CXI - KZ*EX1(J,nxt))*COSBJ - (CZI - KX*EZ1(J,nxt))*SINBJ
RM2 = (CXI - KZ*EX2(J,nxt))*COSBJ - (CZI - KX*EZ2(J,nxt))*SINBJ
RSQ1 = RM1*RM1 + RN*RN
RSQ2 = RM2*RM2 + RN*RN
TB=0.0
IF(RN.NE.0.0) TB=2.0*(ATAN(RM1/RN)-ATAN(RM2/RN))
TC = 2.0 * RN * (RM1/RSQ1 - RM2/RSQ2)
TE = ALOG(RSQ1/RSQ2)
TD = (RN*RN - RM1*RM1)/RSQ1 - (RN*RN - RM2*RM2)/RSQ2
COS2F = 2.0*(COS2BI*(COSBJ*COSBJ - 0.5) + SIN2BI*SINBJ*COSBJ)
SIN2F = 2.0*(SIN2BI*(COSBJ**2 - 0.5) - COS2BI*SINBJ*COSBJ)
TK = TK + TB*KX*KZ
TL = TL + TE
TM = TM + (TD + TA*TE)*COS2F + (TC - TA*TB)*SIN2F
TN = TN + (((1.0-TA)*TB-TC)*COS2F + (TD+(1.0-TA)*TE)*SIN2F)*KX*KZ
TO = TO + (TD + TA*TE)*SIN2F - (TC - TA*TB)*COS2F
TP = TP + (((1.0-TA)*TB-TC)*SIN2F - (TD+(1.0-TA)*TE)*COS2F)*KX*KZ
102 CONTINUE
BMM(I,J) = (TL + TM) * TJ
BMN(I,J) = (TK + TN) * TJ
BNM(I,J) = (TL - TM) * TJ
BNN(I,J) = (TK - TN) * TJ
DM(I,J) = TO * TJ
DN(I,J) = TP * TJ
101 CONTINUE
C ** SKIP FICTITIOUS LOAD CALCULATION DURING PROCESSING INTERIOR POINTS **
C IF(NN.GT.0) GO TO 404
C
C ** DETERMINATION OF FICTITIOUS LOADS BY ITERATION **
C
M = 0
400 DO 401 I = 1,MAXI
QMI = PNM(I)
QNI = PN(I)
DO 402 J = 1,MAXJ
IF(I.EQ.J) GO TO 402
QMI = QMI - DM(I,J)*QM(J) - DN(I,J)*QN(J)
QNI = QNI - BNM(I,J)*QM(J) - BNN(I,J)*QN(J)
402 CONTINUE
DENOM = BNN(I,I)*DM(I,I) - DN(I,I)*BNM(I,I)
QM(I) = (QMI*BNN(I,I) - QNI*DN(I,I))/DENOM
QN(I) = (QNI*DM(I,I) - QMI*BNM(I,I))/DENOM
401 CONTINUE
M = M + 1
IF(M.LT.NCYC) GO TO 400
C
C-----
C
C ***** DETERMINATION OF STRESS COMPONENTS,
C PRINCIPAL STRESSES AND DIRECTION *****
C-----
C
404 CONTINUE
do 500 ii=1,maxi
i=ii
nss=nxt
if(ncal.ne.1) go to 9972
nss=nxt+1
i=nref(ii,nss)

```



```

9972 continue
c DO 500 I = 1,MAXI
  SMI = FPX * 2.0
  SNI = FPZ * 2.0
  SNMI = 0.0
  IF(NN.GT.0.and.ncal.eq.0) GO TO 405
  SMI = 2.0*((FPX-FPZ)* COSB(I,nss) **2 + FPZ)
  SNI = 2.0*((FPX-FPZ)* SINB(I,nss) **2 + FPZ)
  SNMI = 2.0*(FPX-FPZ)*SINB(I,nss) *COSB(I,nss)
  if(nhcal.ge.1)go to 9041
  if(nxt.ne.1.or.ncal.eq.1) go to 9041
  alen=sqrt((ex2(i,nss)-ex1(i,nss))**2+
1 (ez2(i,nss)-ez1(i,nss))**2)
  ensx2(i,nss)=snmi*0.5*alen
  ensz2(i,nss)=sni*0.5*alen
9041 continue
405 DO 501 J = 1,MAXJ
  SNI = SNI - BNM(I,J)*QM(J) - BNN(I,J)*QN(J)
  SMI = SMI - BMM(I,J)*QM(J) - BMN(I,J)*QN(J)
  SNMI = SNMI - DM(I,J)*QM(J) - DN(I,J)*QN(J)
501 CONTINUE
  if(ncal.ne.1) go to 9994
  alen=sqrt((ex2(i,nss)-ex1(i,nss))**2+
1 (ez2(i,nss)-ez1(i,nss))**2)
  ensx2(i,nss)=snmi*0.5*alen
  ensz2(i,nss)=sni*0.5*alen
  go to 500
9994 continue
  SDI = 0.5*(SMI-SNI)
  TAUMAX = 0.5*SQRT(SDI**2 + SNMI**2)
  SIG1(I) = 0.25*(SMI+SNI) + TAUMAX
  SIG3(I) = 0.25*(SMI+SNI) - TAUMAX
  TR = 2.0*TAUMAX + SNMI - SDI
  IF(ABS(TR).LT.1E-8) TR=0.00001
  ALPHA(I) = (180./PI)*ATAN(1.0 + 2.*SDI/TR)
  ES30(I)=SIG1(I)-3.0*SIG3(I)
  SIGM(I)=(SIG1(I)+SIG3(I))/2.0
500 CONTINUE
  if(ncal.eq.1) go to 9996
c
  IF(NN.GT.0) GOTO 611
  WRITE(io,612)
612 FORMAT(1H ///,20X,40HSTRESSES AT CENTRES OF BOUNDARY ELEMENTS)
  GOTO 613
c
611 IF(KSWH.EQ.0) WRITE(io,614) NN
  IF(KSWH.NE.0) WRITE(io,55)
614 FORMAT(1H ///,19X,42HSTRESSES AT INTERIOR POINTS, PARALLEL GRID,
+ 14)
55 FORMAT(1H ///,25X,29HSTRESSES AT ADDITIONAL POINTS)
c
613 WRITE(io,25)
  WRITE(io,26)(I,CX(I,nxt),CZ(I,nxt),SIG1(I),SIG3(I),ALPHA(I),
+ ES30(I),SIGM(I),I=1,MAXI)
25 FORMAT(1H ///,3X,2H I,6X,2HCX,9X,2HCZ,6X,4HSIG1,6X,4HSIG3,5X,
+ 5HALPHA,6X,4HES30,6X,4HSIGM)
26 FORMAT(1H ,14,2f10.2,5f10.1)
c
c * KEYC CONTROLS DISPLACEMENT CALCULATIONS
c
  IF(KEYC.EQ.1) GOTO 205
c
c ** CALCULATE DISPLACEMENTS AT THE BOUNDARY IF ADDITIONAL COORDS.
c ARE SPECIFIED.
c
  IF(NN.EQ.0.AND.KEYD.EQ.1) GOTO 205
  if(keyd.eq.1) go to 205
c
c ** SKIP DISPLACEMENTS
c
  GOTO 575
205 CONTINUE

```

```

C
C-----
C
C ***** DETERMINATION OF DISPLACEMENTS *****
C-----
C
      IF(NN.GT.0) GOTO 607
      WRITE(io,608)
608  FORMAT(1H ///,17X,45HDISPLACEMENTS AT CENTRES OF BOUNDARY ELEMENTS
      1)
      GOTO 609
607  IF(KSWH.EQ.0) WRITE(io,610) NN
      IF(KSWH.NE.0) WRITE(io,60)
610  FORMAT(1H ///,17X,46HDISPLACEMENTS AT INTERIOR POINTS PARALLEL GRID
      + ,14)
      60  FORMAT(1H ///,23X,34HDISPLACEMENTS AT ADDITIONAL POINTS )
C
609  WRITE(io,27)
      27  FORMAT(1H ///,3X,2H I,6X,2HCX,9X,2HCZ,7X,'UX (cm)',8X,'UZ (cm)')
9996  continue
      c   DO 601 I=1,MAXI
          do 601 jjk=1,maxi
              i=jjk
              nss=nxt
              cxi=cx(i,nxt)
              czi=cz(i,nxt)
              if(ncal.ne.1) go to 9997
              nss=nxt+1
              i=nref(jjk,nss)
              cxi=cx(i,nss)
              czi=cz(i,nss)
9997  continue
      c   CXI=CX(I)
      c   CZI=CZ(I)
      c   UX=0.0
      c   UZ=0.0
          ux=cxi*(tw*fpx-rnu/2.0/g*fpz)
          uz=czi*(tw*fpz-rnu/2.0/g*fpx)
          if(nhcal.ge.1)go to 9051
          if(nxt.ne.1.or.ncal.eq.1) go to 9051
          endx2(i,nxt)=ux*cosb(i,nxt)-uz*sinb(i,nxt)
          endz2(i,nxt)=ux*sinb(i,nxt)+uz*cosb(i,nxt)
9051  continue
          UX2=0.0
          UZ2=0.0
C
      DO 602 J=1,MAXJ
      DO 602 KXU=1,KXT(nxt),2
      KX=2-KXU
      DO 602 KZU=1,KZT(nxt),2
      KZ=(2-KZU)*(1-KAS(nxt))+KAS(nxt)*KX
      COSBJ=KX*COSB(J,nxt)
      SINBJ=KZ*SINB(J,nxt)
      RN=(CZI-KX*EZ1(j,nxt))*COSBJ+(CXI-KZ*EX1(j,nxt))*SINBJ
      IF(RN.EQ.0.0) RN=1.0E-8
      LL=KX+KZ-2+10*(I-J)+1000*NN
      IF(LL.EQ.0) RN=SQRT((EX2(i,nss)-EX1(i,nss))**2+(EZ2(i,nss)
      1 -ez1(i,nss))**2)/10000.
      RM1=(CXI-KZ*EX1(j,nxt))*COSBJ-(CZI-KX*EZ1(j,nxt))*SINBJ
      RM2=(CXI-KZ*EX2(j,nxt))*COSBJ-(CZI-KX*EZ2(j,nxt))*SINBJ
      RSQ1=SQRT(RM1*RM1+RN*RN)
      RSQ2=SQRT(RM2*RM2+RN*RN)
      RNO=-KX*EZ1(j,nxt)*COSBJ-KZ*EX1(j,nxt)*SINBJ
      RM10=KZ*EX1(j,nxt)*COSBJ-KX*EZ1(j,nxt)*SINBJ
      RM20=KZ*EX2(j,nxt)*COSBJ-KX*EZ2(j,nxt)*SINBJ
      RSQ10=SQRT(RM10*RM10+RNO*RNO)
      RSQ20=SQRT(RM20*RM20+RNO*RNO)
      IF(RSQ10.LT..001)RSQ10=.001
      IF(RNO.LT..00001.AND.RSQ20.LT..001) RSQ20=.001
      IF(RNO.LT..00001)RNO=0.00001
      TS2=-RN*ALOG(RSQ2/RSQ1)

```

```

TR2=-RN*(ATAN(RM2/RN)-ATAN(RM1/RN))
TT2=TU*(-RM2*ALOG(RSQ2)+RM1*ALOG(RSQ1)+RM2-RM1+TR2)
UM2=TV*(TS2*QN(J)*KX*KZ-(TT2+TR2)*QM(J))
UN2=TV*(TS2*QM(J)-(TT2-RM2+RM1-TR2)*KX*KZ*QN(J))
UZ2=UZ2-UM2*SINBJ+UN2*COSBJ
UX2=UX2+UM2*COSBJ+UN2*SINBJ
602 CONTINUE
C
UX=ux+ux2
UZ=uz+uz2
UX2=-UX2
UZ2=-UZ2
if(nhcal.ge.1) go to 3031
if(ncal.ne.1) go to 9998
endx2(i,nxt+1)=ux*cosb(i,nxt+1)-uz*sinb(i,nxt+1)
endz2(i,nxt+1)=ux*sinb(i,nxt+1)+uz*cosb(i,nxt+1)
go to 601
9998 continue
enbcdx(i,nxt)=ux*cosb(i,nxt)-uz*sinb(i,nxt)
enbcdz(i,nxt)=ux*sinb(i,nxt)+uz*cosb(i,nxt)
c ux=-ux
c uz=-uz
3031 continue
ux9=ux2*100.
uz9=uz2*100.
WRITE(io,28) I,CX1,CZI,UX9,UZ9
28 FORMAT(1H ,I4,2F10.2,f12.4,3x,f12.4)
601 CONTINUE
575 CONTINUE
C
C ** BRANCH TO STARTING POINT IF ADDITIONAL POINTS HAVE BEEN PROCESSED.
C
IF(KSWH.EQ.1) GOTO 9992
if(ncal.eq.0) go to 9961
COS2BI = 1.0
SIN2BI = 0.0
9961 continue
if(nhcal.ge.1) go to 3030
CCC-----
CCC
CCC calculate energy released
CCC-----
if(nexc.eq.1.and.keyc.eq.0) go to 9052
if(nxt.ne.1.or.ncal.eq.1) go to 9052
uii=0.0
umm=0.0
do 9053 kk=1,maxi
umm=umm+0.5*(ensx2(kk,nxt)*endx2(kk,nxt)
1 +ensz2(kk,nxt)*endz2(kk,nxt))
uii=uii+0.5*(ensx2(kk,nxt)*(enbcdx(kk,nxt)
1 -endx2(kk,nxt))+ensz2(kk,nxt)*(enbcdz(kk,nxt)-endz2(kk,nxt)))
9053 continue
nsym=(1+kxt(nxt)/2)*(1+kzt(nxt)/2)
uii=uii*nsym
umm=umm*nsym
write(io,1120)nxt
write(*,1120)nxt
beta=uii/umm
w=2.0*umm*(1.0+beta)
uc=(2.0+beta)*umm
wr=(1.0+beta)*umm
se=(uii/wr)*100.
write(io,1119)uii,umm,w,uc,wr,se
write(*,1119)uii,umm,w,uc,wr,se
9052 continue
C
C ** GENERATION OF GRID POINTS, STRESSES AND DISPLACEMENTS
C DETERMINED BY LOOPING TO 105
C
if(ncal.eq.1) go to 9981
if(nexc.eq.1) go to 9981

```

```

      if(nxt.gt.nexc-1) go to 9981
      nn=1
      maxi=numexc(nxt+1)
      maxj=maxj9(nxt)
      ncal=1
      go to 655
9981  continue
      ncal=0
      nn=0
      umm=0.0
      uii=0.0
      if(nxt.eq.1) go to 9971
      do 9985 ik=1,numexc(nxt)
      kk=nref(ik,nxt)
      umm=umm+0.5*(ensx2(kk,nxt)*endx2(kk,nxt)+
1 ensz2(kk,nxt)*endz2(kk,nxt))
      uii=uii+0.5*(ensx2(kk,nxt)*(enbcdx(kk,nxt)-endx2(kk,nxt)
1 )+ensz2(kk,nxt)*(enbcdz(kk,nxt)-endz2(kk,nxt)))
9985  continue
      nsym=(1+kxt(nxt)/2)*(1+kzt(nxt)/2)
      uii=uii*nsym
      umm=umm*nsym
      write(io,1120)nxt
      write(*,1120)nxt
      beta=uii/umm
      w=2.0*umm*(1.0+beta)
      uc=(2.0+beta)*umm
      wr=(1.0+beta)*umm
      se=(uii/wr)*100.
      write(io,1119)uii,umm,w,uc,wr,se
      write(*,1119)uii,umm,w,uc,wr,se
1119  format(1h ///,7x,'Wk, Um, W, Uc, Wr =',5f10.3,/,7x,'SEISMIC EFFICI
1 ENCY=',F8.1,' %')
1120  format(1h ///,15x,'***** EXCA STAGE NO. =',i3,' ENERGY SUMMARY
1 *****')
9971  continue
      nhcal=nhcal+1
3030  continue
      IF(NN.EQ.NSL(nxt)) GO TO 503
      NN = NN + 1
      IF(NN.GT.1) GO TO 504
      IF(KEY.EQ.0) GOTO 550
      MAXI= (MAXJ-1)/KBAR+1
      DO 560 I=1,MAXI
      K=KBAR*I-(KBAR-1)
      CX(I,nxt) = CX(K,nxt)
      CZ(I,nxt) = CZ(K,nxt)
      SB(I) = SINB(K,nxt)
      CB(I) = COSB(K,nxt)
560  CONTINUE
      IF(KEY.EQ.1) GOTO 565
550  CONTINUE
      MAXI2 = MAXI
      MAXI = 0
      PREX = 100.
      PREY = 100.
      DO 502 I = 1,MAXI2
      REST = SQRT( (CX(i,nxt)-PREX)**2 + (CZ(i,nxt)-PREY)**2 ) - CRIT
      IF( REST.LT.-1E-8 ) GOTO 502
      PREX = CX(i,nxt)
      PREY = CZ(i,nxt)
      MAXI = MAXI + 1
      CX(MAXI,nxt) = CX(i,nxt)
      CZ(MAXI,nxt) = CZ(i,nxt)
      SB(MAXI) = SINB(i,nxt)
      CB(MAXI) = COSB(i,nxt)
502  CONTINUE
565  CONTINUE
504  TQ = DELN(nxt)*NN
      DO 505 I = 1,MAXI
      CX(i,nxt) = CX(i,nxt) + SB(i)*TQ
      CZ(i,nxt) = CZ(i,nxt) + CB(i) *TQ

```

```

505 CONTINUE
C
C ** REPEAT FOR ANOTHER PARALLEL GRID POINTS **
C
      GOTO 655
C
c 503 IF(KEYD.EQ.0) GOTO 31415
503  if(keyd.eq.0) go to 9992
      KSWH=1
      WRITE(io,220)
220  FORMAT(1H1///// ' STRESSES AND DISPLACEMENTS AT ADDITIONAL POINTS',
+ /1X,47(1H-),/)
      NN = NN + 1
      I=0
1003 continue
      if(nopt.eq.2) write(*,3020)nxt
3020 format(1x,'STRESSES AND DISPLACEMENTS AT ADDITIONAL POINTS',
1 ' AT EXCAVATION STAGE No. =',i3,/,1x,
1 ' INPUT NBS CX1 CZ1 CX2 CZ2 ?',/,1x,
1 'NBS -- No. OF POINTS FOR STRESSES AND DISPLACEMENTS CALCULATIONS',
1 /,1x,'WHEN NBS > 99999 INPUT TERMINATED',
1 /,1x,'CX1,CZ1,CX2,CZ2 -- THE COORDINATES OF THE STARTING POINTS',
1 ' AND ENDING POINTS OF THE LINE SEGMENT ',/,1x,
1 'WHERE STRESSES AND DISPLACEMENT ARE CALCULATED. ')
      if(nopt.eq.2)write(*,5010)
5010 format(1x,'NBS, CX1, CZ1, CX2, CZ2?')
      READ(in,*) NBS,CX1,CZ1,CX2,CZ2
      if(nopt.eq.2) write(is,*)nbs,cx1,cz1,cx2,cz2
230  FORMAT(15,4F10.0)
C
C ** MET END OF DATA MARKER NBS>=9999 **
C
      IF (NBS.GE.9999)GO TO 655
      IF(NBS.EQ.0)GOTO 1111
      JSUM=I+NBS
      IF(JSUM.GT.LMTARA)GOTO 655
      DX=(CX2-CX1)/FLOAT(NBS)
      DZ=(CZ2-CZ1)/FLOAT(NBS)
      DO 1001 JJ=1,NBS
      I=I+1
      MAXI=I
      CMNM=FLOAT(JJ)-0.5
      CX(i,nxt)=CX1+CMNM*DX
      CZ(i,nxt)=CZ1+CMNM*DZ
1001 CONTINUE
      GOTO 1002
1111 I=I+1
      MAXI=I
      CX(i,nxt)=CX1
      CZ(i,nxt)=CZ1
1002 IF(I.LT.LMTARA) GOTO 1003
      STOP
9992 continue
      go to 31415
      END

```

